UNIVERSITY OF AMSTERDAM

UvA-DARE (Digital Academic Repository)

A local VE-cadherin and Trio-based signaling complex stabilizes endothelial junctions through Rac1

Timmerman, I.; Heemskerk, N.; Kroon, J.; Schaefer, A.; van Rijssel, J.; Hoogenboezem, M.; van Unen, J.; Goedhart, J.; Gadella, T.W.J.; Yin, T.; Wu, Y.; Huveneers, S.; van Buul, J.D.

DOI
10.1242/jcs.168674

Publication date
2015

Document Version
Final published version

Published in
Journal of Cell Science

Link to publication

Citation for published version (APA):
Timmerman, I., Heemskerk, N., Kroon, J., Schaefer, A., van Rijssel, J., Hoogenboezem, M., van Unen, J., Goedhart, J., Gadella, T. W. J., Yin, T., Wu, Y., Huveneers, S., & van Buul, J. D. (2015). A local VE-cadherin and Trio-based signaling complex stabilizes endothelial junctions through Rac1. *Journal of Cell Science*, *128*(16), 3041-3054. https://doi.org/10.1242/jcs.168674

General rights
It is not permitted to download or to forward/distribute the text or part of it without the consent of the author(s) and/or copyright holder(s), other than for strictly personal, individual use, unless the work is under an open content license (like Creative Commons).

Disclaimer/Complaints regulations
If you believe that digital publication of certain material infringes any of your rights or (privacy) interests, please let the Library know, stating your reasons. In case of a legitimate complaint, the Library will make the material inaccessible and/or remove it from the website. Please Ask the Library: https://uba.uva.nl/en/contact, or a letter to: Library of the University of Amsterdam, Secretariat, P.O. Box 19185, 1000 GD Amsterdam, The Netherlands. You will be contacted as soon as possible.
UvA-DARE is a service provided by the library of the University of Amsterdam (https://dare.uva.nl)

Download date:15 Sept 2026

© 2015. Published by The Company of Biologists Ltd | Journal of Cell Science (2015) 128, 3041-3054 doi:10.1242/jcs.168674

RESEARCH ARTICLE

A local VE-cadherin and Trio-based signaling complex stabilizes endothelial junctions through Rac1

Ilse Timmerman[1], Niels Heemskerk[1], Jeffrey Kroon[1], Antje Schaefer[1], Jos van Rijssel[1], Mark Hoogenboezem[1], Jakobus van Unen[2], Joachim Goedhart[2], Theodorus W. J. Gadella, Jr[2], Taofei Yin[3], Yi Wu[3], Stephan Huveneers[1] and Jaap D. van Buul[1,*]

ABSTRACT

Endothelial cell–cell junctions maintain a restrictive barrier that is tightly regulated to allow dynamic responses to permeability-inducing angiogenic factors, as well as to inflammatory agents and adherent leukocytes. The ability of these stimuli to transiently remodel adherens junctions depends on Rho-GTPase-controlled cytoskeletal rearrangements. How the activity of Rho-GTPases is spatio-temporally controlled at endothelial adherens junctions by guanine-nucleotide exchange factors (GEFs) is incompletely understood. Here, we identify a crucial role for the Rho-GEF Trio in stabilizing junctions based around vascular endothelial (VE)-cadherin (also known as CDH5). Trio interacts with VE-cadherin and locally activates Rac1 at adherens junctions during the formation of nascent contacts, as assessed using a novel FRET-based Rac1 biosensor and biochemical assays. The Rac-GEF domain of Trio is responsible for the remodeling of junctional actin from radial into cortical actin bundles, a crucial step for junction stabilization. This promotes the formation of linear adherens junctions and increases endothelial monolayer resistance. Collectively, our data show the importance of spatio-temporal regulation of the actin cytoskeleton through Trio and Rac1 at VE-cadherin-based cell–cell junctions in the maintenance of the endothelial barrier.

KEY WORDS: Trio, VE-cadherin, GEF, Rac1, Endothelium

INTRODUCTION

The endothelium lining the vessel wall forms a major barrier between the circulation and the surrounding tissues, preventing plasma leakage. Endothelial adherens junctions, comprising the vascular endothelial (VE)-cadherin–catenin complex, function to maintain the monolayer integrity. VE-cadherin-based cell–cell junctions are dynamic and remodeled during processes such as leukocyte extravasation or angiogenesis, and also during homeostasis (Dejana, 2004; Vestweber et al., 2009). Therefore, cell–cell junctions are tightly regulated. The extracellular domain of VE-cadherin mediates homophilic Ca^{2+}-dependent adhesion, whereas β-catenin (also known as CTNNB1) indirectly links the intracellular domain of VE-cadherin to the actin cytoskeleton through α-catenin (of which there are three isoforms, known as CTNNA1–3) (Lampugnani et al., 1992; Navarro et al., 1995). Additional F-actin-binding and regulating proteins are recruited to modify the strength of VE-cadherin-based adhesions (Bershadsky, 2004; Huveneers and de Rooij, 2013).

Changes in the actin cytoskeleton have a major impact on the morphology and stability of VE-cadherin-based cell–cell junctions (Hultin et al., 2014; Noda et al., 2010; Phng et al., 2015; Sauteur et al., 2014; Schulte et al., 2011), in part by altering the magnitude and direction of the forces that are exerted on cell–cell junctions (Oldenburg and de Rooij, 2014). Distinct types of cell–cell junctions exist depending on the organization of the junction-associated actin cytoskeleton. Destabilization of cell–cell junctions in response to permeability-inducing factors, such as thrombin and vascular endothelial growth factor (VEGF), is associated with the presence of radial contractile actin bundles that terminate at cell–cell junctions. These remodeling junctions have a discontinuous morphology and a different molecular composition. In this study, we will refer to these junctions as focal adherens junctions (FAJs) to make a distinction from other junction conformations (Huveneers et al., 2012). By contrast, cell–cell adhesion stabilization is supported through cortical actin bundles that run parallel to the cell–cell junction (Noda et al., 2010). The presence of thick cortical actin bundles near to junctions correlates with the appearance of stable, continuous junctions (Oldenburg and de Rooij, 2014). Interestingly, homophilic ligation of cadherins has been reported to directly recruit and activate actin regulators that reorganize the cytoskeleton, indicative of bidirectional interplay (Huveneers and de Rooij, 2013; Kovacs et al., 2002; Lambert et al., 2002).

Members of the Rho family of GTPases are of key importance in the control of actomyosin organization. In epithelial cells, the small GTPase Rac1 initiates cell–cell adhesion by promoting Arp2/3-based membrane protrusions and eventually stabilizes these contacts by promoting the formation of cortical actin bundles adjacent to the junction (Yamada and Nelson, 2007; Yamazaki et al., 2007; Zhang et al., 2005). However, junction formation in endothelium and epithelium does not follow the exact same mechanism. Hoelzle and Svitkina, for example, show that endothelial cells use lamellipodia as the initial contact and then transform these into filopodia-like bridges that develop into nascent VE-cadherin-based junctions (Hoelzle and Svitkina, 2012). Moreover, Rac1 is reported to be required for barrier maintenance, but to be also needed for VE-cadherin endocytosis and reactive oxygen species (ROS)-mediated loss of VE-cadherin-mediated cell–cell contacts (Gavard and Gutkind, 2006; Spindler et al., 2010; van Wetering et al., 2002). Thus, Rac1 controls signaling mechanisms that have opposing effects on endothelial cell–cell junctions, suggesting a need for finely balanced spatial and temporal regulation of its activity.

[1]Department of Molecular Cell Biology, Sanquin Research and Landsteiner Laboratory, Academic Medical Center, University of Amsterdam, Amsterdam 1066 CX, The Netherlands. [2]Swammerdam Institute for Life Sciences, Section of Molecular Cytology, van Leeuwenhoek Centre for Advanced Microscopy, University of Amsterdam, Amsterdam 1098 XH, The Netherlands. [3]Center for Cell Analysis and Modelling, University of Connecticut Health Center, Farmington, CT 06032, USA.

*Author for correspondence (j.vanbuul@sanquin.nl)

Received 20 January 2015; Accepted 22 June 2015

Journal of Cell Science (2015) 128, 3041-3054 doi:10.1242/jcs.168674

A possible mechanism for the spatio-temporal activation of Rac1 at cell–cell junctions is through localized activation of guanine-nucleotide exchange factors (GEFs); factors that activate small GTPases by promoting the exchange of bound GDP for GTP (Rossman et al., 2005). It is still unclear which of the many identified Rac-GEFs that function in endothelial cells control VE-cadherin-based cell–cell junctions. Previous work from our group has implicated the Rac1-GEF Trio in primary human endothelium as an important regulator of the transendothelial migration of leukocytes (van Rijssel et al., 2012b). Because we have previously observed that Trio localizes at endothelial cell–cell junctions, we further studied whether Trio has a role in the regulation of endothelial junctions. Here, we show that Trio binds to VE-cadherin during junction (re-)formation, locally activates Rac1 and thereby promotes the transition from nascent-to-stable VE-cadherin-based adhesion.

RESULTS

Trio controls endothelial cell–cell junction organization and barrier function

Our previous work has identified a role for the endothelial GEF Trio in inflammation and leukocyte diapedesis. Also we observed that Trio-deficient endothelial cells form cell–cell junctions that are organized in a less linear manner (van Rijssel et al., 2012b, 2013). To investigate the role of Trio in endothelial junction regulation, we silenced the expression of Trio in endothelial cells by using short hairpin RNAs (shRNAs). Trio-deficient cells showed a larger phenotype when spread compared with control cells. Using real-time imaging of green fluorescent protein (GFP)-tagged VE-cadherin (VE-cadherin–GFP), we found that cell–cell junctions of Trio-deficient endothelial cells (marked by TagRFP) remained unstable compared with those in cells that had been transfected with a control shRNA (shCTRL) (Fig. 1A; supplementary material Movie 1). Detailed analysis showed that both control and Trio-deficient endothelial cells displayed linear and irregular cell–cell junctions (Fig. 1B). These irregular junctions have been previously described and named focal adherens junctions (FAJ), which are sites of junction remodeling (Huveneers et al., 2012) (Fig. 1B). We quantified the total length of FAJs in single cells that had been grown in monolayers by using VE-cadherin as a marker for cell–cell junctions and compared the total lengths of the FAJs to the total junction length, according to the quantification approach described previously by Wilson and colleagues (2013) (supplementary material Fig. S1B). This revealed that endothelial cells that lacked Trio showed increased total lengths of FAJs (Fig. 1B; supplementary material Fig. S1B). Moreover, studying the total lengths of the FAJs in cells over time revealed that a large portion of the junctions between Trio-deficient cells remained organized as FAJs (supplementary material Fig. S1B). We wish to note that some of the FAJs in control cells showed a thicker phenotype, whereas FAJs from Trio-deficient cells showed a more focal phenotype. Both phenotypes were quantified as FAJs (supplementary material Fig. S1B). This indicates that cell–cell junctions in Trio-deficient cells are unstable and continuously dis- and re-assemble.

To test whether Trio deficiency has functional consequences for monolayer barrier function, we measured the electrical resistance of endothelial monolayers using electrical cell–substrate impedance sensing (ECIS). We found that silencing Trio, using two independent shRNA constructs, strongly reduced endothelial cell monolayer resistance compared with that of control cells, indicating that a lack of Trio reduces junction integrity (Fig. 1C). Also, permeability was increased in Trio-deficient endothelial cells, as assessed by determining the leakage of fluorescently-labeled dextran across Transwell filters (supplementary material Fig. S1C). Thus, these data show that Trio is required for barrier function by regulating endothelial cell–cell junction organization.

Trio is a Rho-GEF comprising three catalytic domains – two GEF domains (to activate small GTPases) and a serine/threonine kinase domain (Fig. 1D). The N-terminal GEF domain (GEF1) activates Rac1 and RhoG, whereas the C-terminal GEF domain (GEF2) activates RhoA (Blangy et al., 2000; Debant et al., 1996; van Rijssel et al., 2012a). Using the GEF1 inhibitor ITX3, we showed that the activity of GEF1 is required to maintain endothelial resistance (supplementary material Fig. S1D). To further test whether Trio activity is involved in the regulation of the barrier function of the endothelium, we rescued the impaired resistance of endothelial cells that expressed shRNAs against Trio (shTrio) by expressing the N-terminus of Trio (TrioN), which includes the GEF1 domain and of which the expression is not targeted by the shRNA (van Rijssel et al., 2012a). The endothelial barrier defect of Trio-deficient cells was readily rescued upon expression of TrioN (Fig. 1E; supplementary material Fig. S1E). Moreover, TrioN overexpression in wild-type human umbilical vein endothelial cells (HUVECs) enhanced endothelial monolayer resistance, whereas overexpression of the C-terminus of Trio (TrioC), which includes the GEF2 domain, did not (Fig. 1F; supplementary material Fig. S1E). Inhibiting Rac1 by using EHT-1864 (Onesto et al., 2008) in cells that expressed TrioN additionally showed that TrioN promoted endothelial electrical resistance through the activation of Rac1 (Fig. 1G). In order to investigate whether the TrioN-mediated increase in resistance involves VE-cadherin, we used a VE-cadherin-blocking antibody. This antibody efficiently reduces VE-cadherin-mediated barrier function (Corada et al., 2001; van Buul et al., 2005). When endothelial cells were pretreated with this antibody, overexpression of TrioN in Trio-deficient cells failed to rescue the drop in electrical resistance, indicating that VE-cadherin is involved in Trio-mediated barrier enhancement (Fig. 1H). Taken together, these data indicate that Trio is required to maintain the endothelial barrier function in a Rac1-dependent manner.

Because the junctions of Trio-deficient endothelial cells rapidly dis- and re-assemble, we next focused on the role of Trio during junction remodeling and used the permeability mediator thrombin to induce actomyosin-dependent junction disruption (Huveneers et al., 2012; van Hinsbergh and van Nieuw Amerongen, 2002). Thrombin rapidly destabilized cell–cell junctions (within 5 min), and cell–cell junctions recovered after 30 min, resulting in full restoration of the integrity of the endothelial cell monolayer after approximately 2–3 h (supplementary material Movie 2). Interestingly, overexpression of TrioN promoted the formation of linear junctions in endothelial cells and prevented the thrombin-induced loss of cell–cell contact (Fig. 2A; supplementary material Movie 3), indicating that Trio promotes the stabilization of cell–cell junctions. Conversely, ECIS analyses showed that depletion of Trio delayed the recovery of barrier function after treatment with thrombin (Fig. 2B). Quantification of the recovery after 3 h of treatment with thrombin showed that the control cells reached maximal recovery, whereas in Trio-deficient cells, the recovery was significantly delayed to 59% of the maximal recovery. To investigate whether, during recovery, Trio directly controls VE-cadherin-based junction assembly, we performed real-time imaging of VE-cadherin–GFP in Trio-depleted and control endothelial cells. Under control conditions, thrombin rapidly remodeled and disrupted VE-cadherin-positive cell–cell junctions, which was followed by the reassembly of cell–cell contacts and the

Journal of Cell Science

Journal of Cell Science (2015) 128, 3041-3054 doi:10.1242/jcs.168674

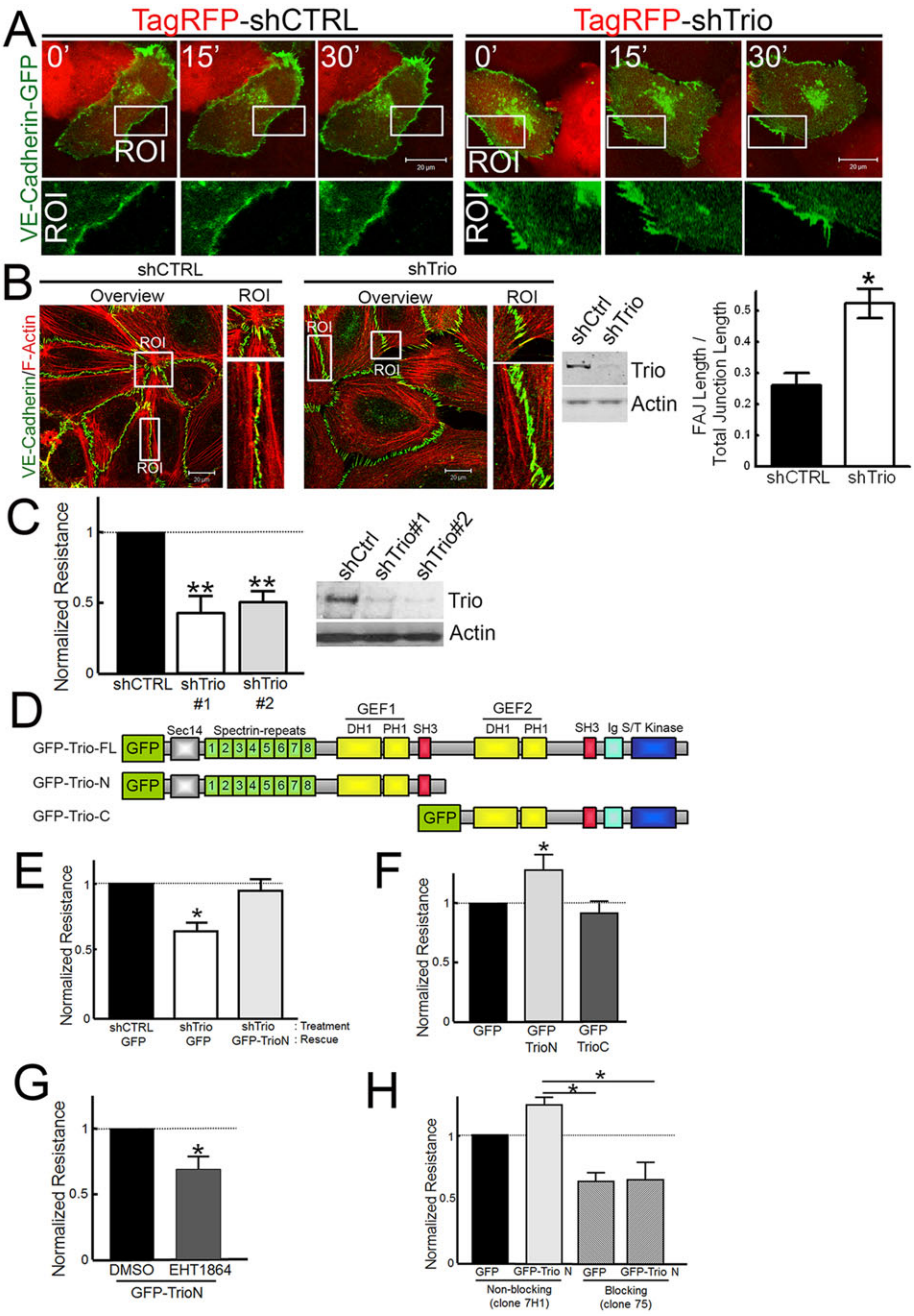

Fig. 1. Trio promotes endothelial barrier function. (A) Endothelial cells are transfected with a TagRFP-labeled control shRNA (TagRFP–shCTRL) or a TagRFP-labeled shRNA against Trio (TagRFP-shTrio) (red) and VE-cadherin–GFP (green). The dynamics of cell–cell junctions were followed over time as indicated (min). Regions of interest (ROI) show VE-cadherin–GFP distribution over time. (B, left) HUVECs were transduced with shCTRL or shTrio and stained as indicated. (Middle) Western blots show Trio knockdown. (Right) The FAJ length versus the total junction length was quantified. Scale bars: 20 µm. (C) Endothelial cells were transduced with control or two different shRNAs against Trio, and electrical resistance was monitored by using ECIS. The bar graph represents electrical resistance one day after seeding. The western blot shows Trio knockdown. (D) Overview of GFP–Trio constructs – full-length Trio (GFP–TrioFL), the N-terminus of Trio containing GEF1 (GFP–TrioN) and the C-terminus containing GEF2 (GFP–TrioC). (E) Endothelial cells were transduced with Trio or control shRNA, followed after 2 days by infection with adenovirus expressing GFP or GFP–TrioN. The bar graph represents the electrical resistance. (F) Endothelial cells were transduced with adenovirus encoding GFP–TrioN or GFP–TrioC. (G) Endothelial cells were transduced with adenovirus encoding GFP–TrioN. Rac1 activity was inhibited by using 50 mM EHT-1864. (H) Endothelial cells expressing GFP or GFP–TrioN were grown to confluence on electrode arrays. One day after cell seeding, a non-blocking (clone 7H1) or a VE-cadherin-blocking (clone 75) antibody was added (6.25 µg/ml). All experiments were performed at least three times. Data are mean±s.e.m. *P<0.05; **P<0.01.

formation of linear junctions (Fig. 2C; supplementary material Movie 4). In Trio-deficient cells, cell–cell junctions were remodeled likewise, which was followed by the reassembly of the junctions. However, newly formed VE-cadherin-based junctions remained unstable and rapidly disassembled again (Fig. 2C; supplementary material Movie 4). Quantification of interendothelial gaps based on differential interference contrast (DIC) imaging analyses after 90 min of exposure to thrombin showed significantly larger gaps in Trio-deficient cells compared with control cells (Fig. 2C; supplementary material Fig. S1F). Thus, Trio is required for stabilization of VE-cadherin-based cell–cell junctions.

Trio localizes at endothelial cell–cell junctions

To further assess the role of Trio in the regulation of endothelial cell–cell junctions, we focused on the subcellular distribution of Trio. Owing to the lack of proper antibodies to detect endogenous Trio in immunofluorescence analyses, we transfected GFP–Trio full length (TrioFL) into primary endothelial cells and observed that Trio localized at cell–cell junctions (Fig. 3A). By expressing different Trio truncation mutants, we found that TrioN but not TrioC localized at cell–cell junctions (Fig. 3A). This indicates that the N-terminus of Trio – encoding the Sec14 domain, spectrin repeats, and the Rac1 and RhoG GEF1 domain – is required for the targeting of Trio to cell–cell junctions. We next examined the localization of Rac1 and RhoG, and expressed the constitutively active forms of these GTPases in endothelial cells. We found that active Rac1, but not RhoG, colocalized with VE-cadherin, indicating that Rac1 is involved in regulating endothelial cell–cell contacts downstream of Trio (supplementary material Fig. S1G).

To test whether VE-cadherin is necessary for Trio localization at cell–cell junctions, we used Chinese hamster ovary (CHO) cells, which normally lack endogenous cadherin expression. We found

Journal of Cell Science (2015) 128, 3041-3054 doi:10.1242/jcs.168674

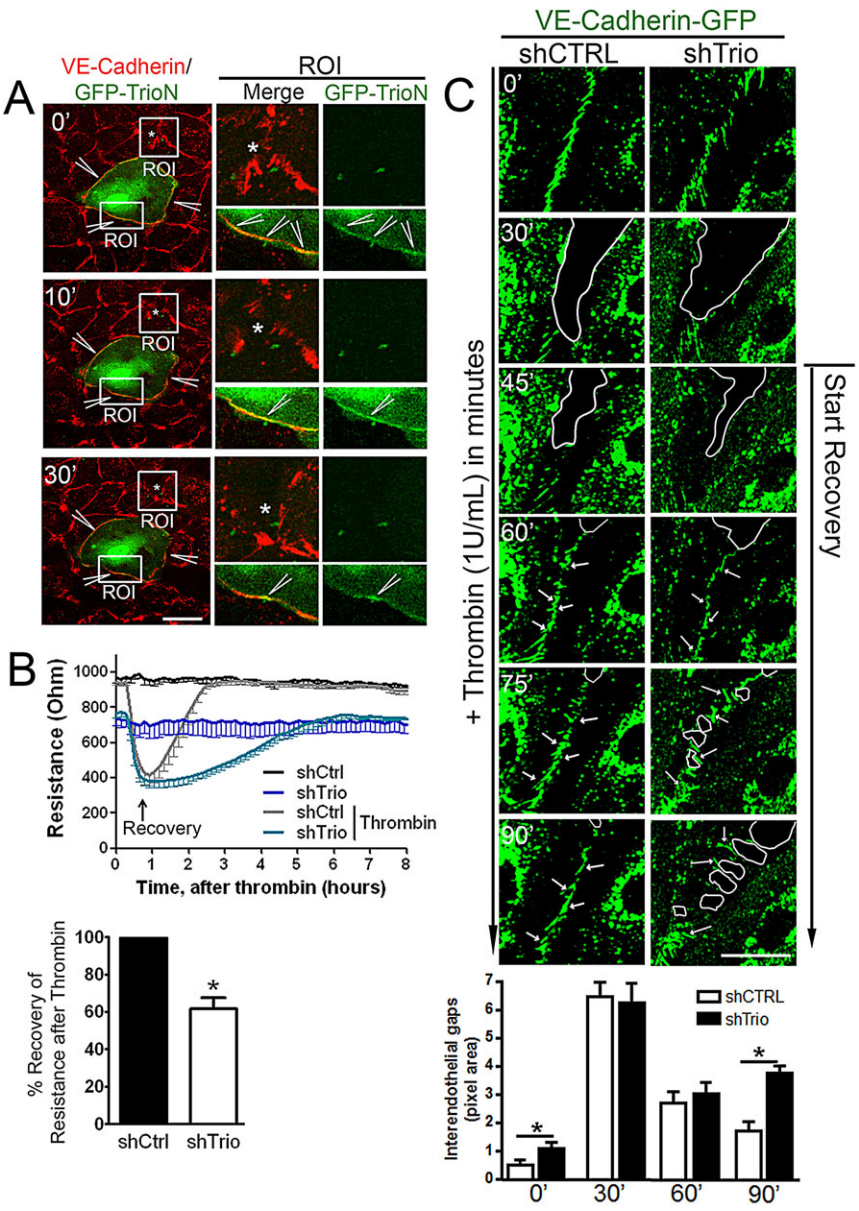

Fig. 2. Trio is required for efficient cell–cell junction recovery. (A) Still images and ROIs from time-lapse recordings (supplementary material Movie 3) showing linear stable cell–cell junctions (arrowheads) in GFP–TrioN-expressing cells, 10–30 min after stimulation with thrombin, whereas a large proportion of cell–cell junctions in non-transfected cells are disrupted (asterisks). VE-cadherin is visualized using an AlexaFluor-647-conjugated antibody. (B) Endothelial cells were transfected with control shRNA (shCtrl, black line) or shRNAs against Trio (shTrio, dark blue line) and grown to confluence on fibronectin-coated electrode arrays. At time point 0, cells were incubated with (dashed line) or without (solid line) thrombin. Resistance was monitored over time by ECIS. Arrow indicates the starting point of the recovery phase. The bar graph represents the percentage recovery of the endothelial monolayer resistance after thrombin at time points when control monolayers had been completely restored. (C) Still images of the time-lapse recording (at the indicated times, min) of thrombin-stimulated control or Trio-depleted endothelial cells expressing VE-cadherin–GFP. See also the corresponding supplementary material Movie 4, which is representative of multiple experiments. Arrows indicate the formation of cell–cell junctions during the recovery phase, indicated by arrows in the panels on the right, and white lines indicate gaps appearing in Trio-deficient cells. Analysis of interendothelial gaps based on DIC imaging showed increased gaps in Trio-deficient cells after treatment with thrombin. All experiments were repeated three times. Data are mean± s.e.m. *P<0.05. Scale bars: 20 µm (A); 10 µm (C).

that Myc-tagged TrioFL only localized at cell–cell contacts when VE-cadherin was co-expressed (Fig. 3B). Additionally, silencing VE-cadherin in endothelial cells prevented Trio localization at cell–cell junctions (Fig. 3C; supplementary material Fig. S1H). Interestingly, silencing VE-cadherin did not prevent β-catenin from localizing at cell–cell junctions. Previous work from Dejana and colleagues shows that under these conditions, N-cadherin localizes at cell–cell junctions (Navarro et al., 1998). Thus, these experiments show that Trio localization at cell–cell contacts depends specifically on the presence of VE-cadherin.

Trio interacts with VE-cadherin

We next investigated whether Trio interacts with the VE-cadherin–catenin complex. Therefore, immunoprecipitation of endogenous Trio from endothelial cell lysates was analyzed by western blotting. These experiments revealed that Trio associates with the VE-cadherin complex, but not with N-cadherin (also known as CDH2), PECAM-1, VEGFR-2 or the tight junction protein ZO-1 (Fig. 4A). Of interest, inhibition of Trio-GEF1 activity using ITX3 did not dissociate VE-cadherin from Trio (supplementary material Fig. S1I), demonstrating that the interaction did not depend on the activity of GEF1. To determine which component of the VE-cadherin complex is required for the interaction with Trio, we used several VE-cadherin truncation mutants and α-catenin fusion proteins to examine the capacity to bind to Trio in cells (Noda et al., 2010) (Fig. 4B). All VE-cadherin–GFP mutants, as well as wild-type VE-cadherin–GFP, localized to cell–cell contacts (Noda et al., 2010). Western blot analysis of immunoprecipitation of these VE-cadherin mutants revealed that Trio has the strongest binding to the full-length VE-cadherin construct (Fig. 4C). The interaction of Trio with the VE-cadherin complex was reduced in the absence of the β-catenin-binding domain (VEΔβ–GFP), as well as when the complete cytoplasmic domain of VE-cadherin was replaced by full-length α-catenin (VEΔC-α–GFP) or α-catenin that lacked the N-terminal β-catenin-binding domain (VEΔC-αΔN–GFP) (Fig. 4C). Because β-catenin co-precipitated with VEΔC-α–GFP and not with VEΔβ–GFP, taken together with the localization studies presented in Fig. 3C, these results indicate that Trio interacts

Journal of Cell Science

Journal of Cell Science (2015) 128, 3041-3054 doi:10.1242/jcs.168674

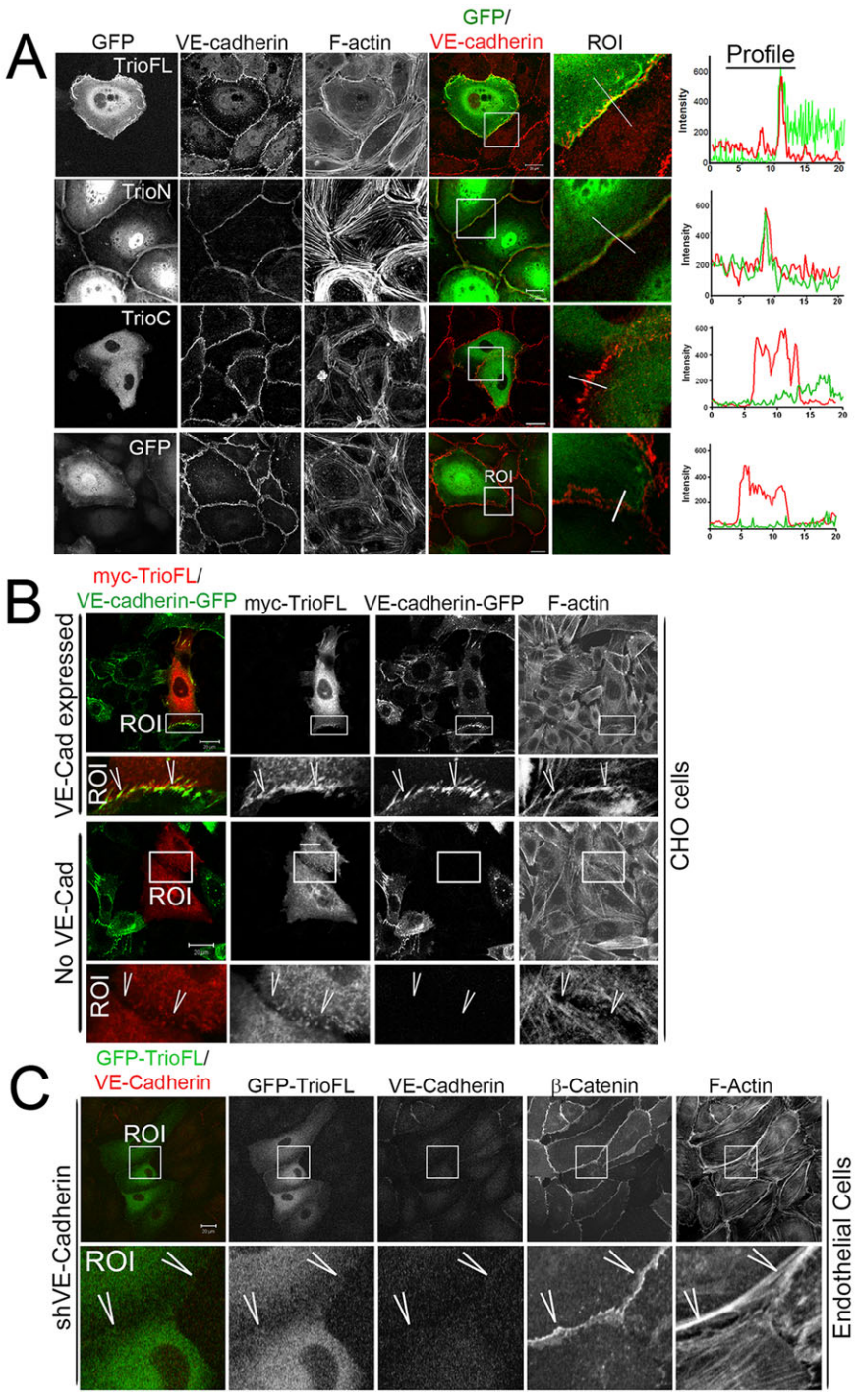

Fig. 3. Trio localizes at endothelial cell–cell contacts. (A) Endothelial cells were transfected with GFP–TrioFL, GFP–TrioN or GFP–TrioC and stained as indicated. ROIs show colocalization between Trio and VE-cadherin. The profile shows the fluorescence intensity of VE-cadherin (red) and GFP proteins (green) according to the line present in the ROI. (B) CHO cells were transfected with Myc-TrioFL and transduced with adenovirus containing VE-cadherin–GFP. Cells were stained as indicated. ROIs (enlarged in the rectangular panels) show that Myc–TrioFL localization at cell–cell contacts depends on VE-cadherin expression. Arrowheads indicate cell–cell contact areas. (C) Endothelial cells were silenced for VE-cadherin and transfected with GFP–TrioFL, and then stained as indicated. ROIs show no localization of Trio at VE-cadherin-deficient cell–cell contacts, but do show β-catenin. Arrowheads indicate cell–cell contact areas. Scale bars: 20 µm.

with VE-cadherin through a region in the intermediate domain that is proximal to the β-catenin-binding domain.

To study whether Trio directly interacts with VE-cadherin, we designed two peptides that encode the intermediate domain of human VE-cadherin (Fig. 4D). Precipitation experiments from cell lysates showed that Trio has a higher affinity for the region of VE-cadherin that partially overlapped with the β-catenin-binding site (amino acid residues 726–765; Fig. 4E), as compared with the region comprising amino acid residues 697–735. Because only TrioN colocalized with VE-cadherin (Fig. 3A; supplementary material Fig. S1J), and co-immunoprecipitation studies between VE-cadherin and different Trio mutants showed strong binding of TrioN to endogenous VE-cadherin (Fig. 4F), we focused on the N-terminal spectrin repeats – known as protein–protein-binding regions – as potential binding sites on Trio for VE-cadherin (Djinovic-Carugo et al., 2002). Using GST-fusion constructs of Trio spectrin repeats 1–4 and 5–8, we found that the VE-cadherin peptide directly associated with spectrin repeats 5–8, whereas a scrambled peptide did not (supplementary material Fig. S2A,B). Further analysis showed that VE-cadherin directly associated with the spectrin repeats 5–6 through its intracellular region at residues 726–765 (Fig. 4G; supplementary material Fig. S2B). These data show that Trio might directly interact with the intracellular tail of VE-cadherin.

Journal of Cell Science

Journal of Cell Science (2015) 128, 3041-3054 doi:10.1242/jcs.168674

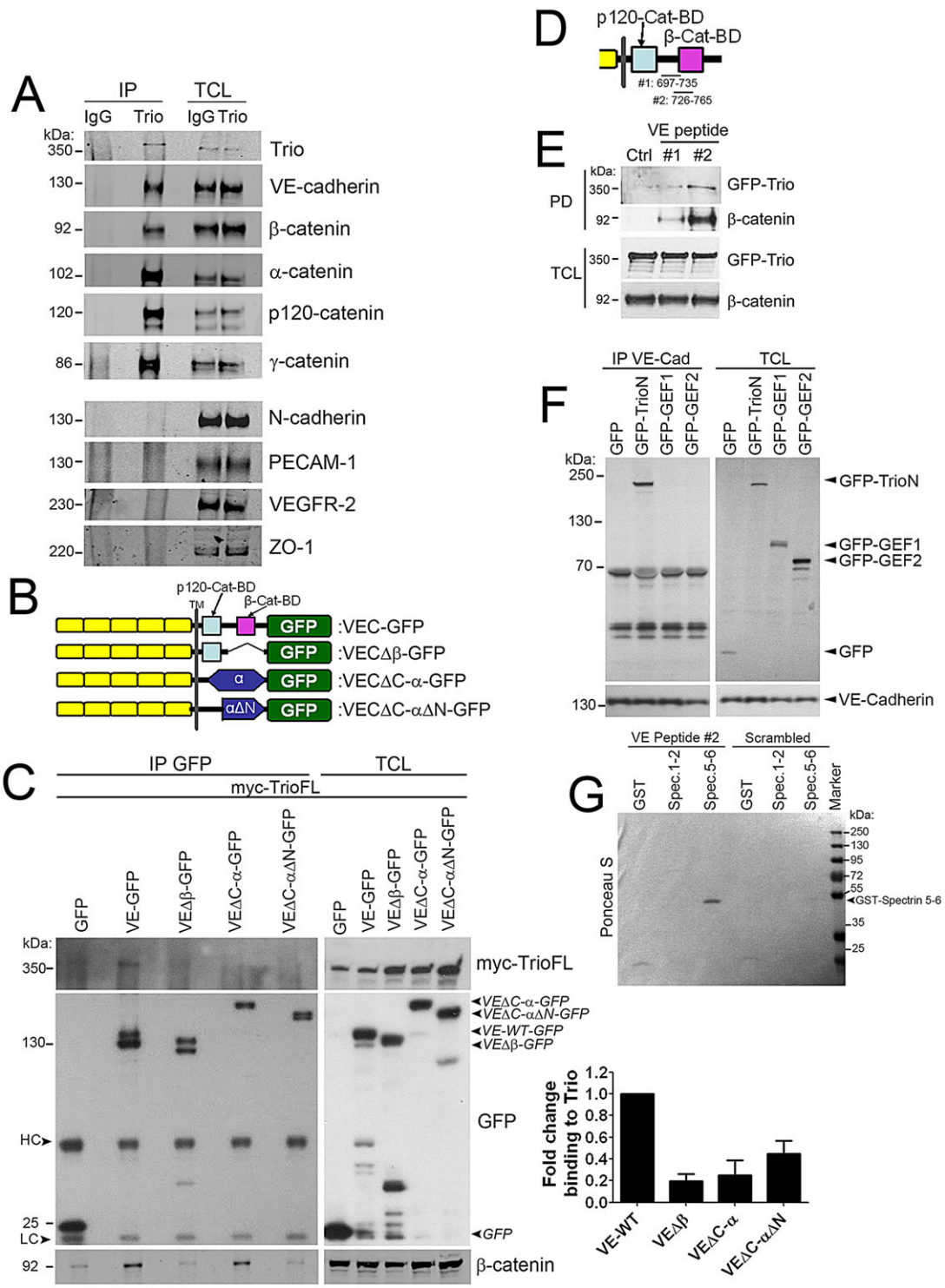

Fig. 4. Interaction of Trio with VE-cadherin. (A) Trio immunoprecipitation (IP) from endothelial cell lysates were analyzed by western blotting. VE-cadherin and the catenins were precipitated, whereas N-cadherin, PECAM-1, VEGFR2 and ZO-1 were not. (B) Overview of VE-cadherin constructs. VEΔβ–GFP, deletion of β-catenin-binding domain; VEΔC-α–GFP, cytoplasmic domain is replaced with α-catenin; VEΔC-αΔN–GFP, cytoplasmic domain is replaced with α-catenin lacking the N-terminal β-catenin-binding domain. (C) Cos7 cells were transfected with Myc-tagged TrioFL, and wild-type VE-cadherin–GFP (VE–GFP) or a VE-cadherin mutant, as indicated. VE-cadherin–GFP was immunoprecipitated by using an antibody against GFP (IP GFP), and the binding of Myc–TrioFL was determined by western blotting. The panel on the right shows the quantification of three independent experiments and the fold-change in binding of VE mutants to Trio compared with VE–wt-binding to Trio. Data are mean±s.e.m. HC, heavy chain; LC, light chain; TCL, total cell lysate. (D) Illustration of the VE-cadherin peptides #1 and #2 used. BD, binding domain; Cat, catenin. (E) HEK293 cells were transfected with GFP–TrioFL and lysed. Specific biotin-tagged peptides, encoding regions of the VE-cadherin cytoplasmic tail as indicated, were used to pull down (PD) GFP–Trio. VE-cadherin peptide (VE peptide) #2 efficiently precipitated TrioFL as well as β-catenin. (F) HUVECs were transfected with GFP–Trio-mutants as indicated, and VE-cadherin (VE-Cad) was immunoprecipitated. Western blot shows interaction of VE-cadherin with TrioN but not with GEF1, GEF2 or GFP. Panels on the right show protein expression in total cell lysates (TCL). (G) VE-cadherin peptide #2 was co-incubated with GST-tagged spectrin repeats (Spec.) as indicated. Western blot analysis shows that Trio spectrin repeats 5–6 interacted with VE peptide #2 and not with the scrambled peptide. Experiments were performed three times independently.

Journal of Cell Science

Journal of Cell Science (2015) 128, 3041-3054 doi:10.1242/jcs.168674

Trio dynamically interacts with VE-cadherin

We next questioned whether the Trio–VE-cadherin interaction is regulated during assembly, stabilization and remodeling of junctions. Because most junctions are stabilized in confluent monolayer cultures, we first tested whether the interaction of Trio with the VE-cadherin–catenin complex is confluence dependent. Trio immunoprecipitation was performed using cell lysates of endothelial monolayers that had been lysed 1 day after plating (recently confluent) and of monolayers that had been lysed 6 days after plating (long confluent) (Fig. 5A). Immunoprecipitates of Trio contained considerably more VE-cadherin and β-catenin when obtained from cells that had been lysed 1 day after plating as compared with those of lysates from cells that had been lysed 6 days after plating. Note that we corrected for total protein concentration – i.e. similar amounts of total Trio and VE-cadherin protein were present in the cell lysates used for immunoprecipitation. Thus, the binding of Trio to the VE-cadherin complex depends on monolayer confluence; binding is reduced when junction stability is increased.

To study whether the Trio–VE-cadherin interaction is regulated during nascent cell–cell junction assembly, the interaction was analyzed in cells during a Ca^{2+}-switch assay. Confluent endothelial monolayers were treated with the Ca^{2+} chelator ethylene glycol tetraacetic acid (EGTA), disrupting adherens junctions, followed by a washout and re-addition of Ca^{2+} to restore cell–cell contact. Immunoprecipitation studies showed that the interaction of Trio with VE-cadherin had significantly increased only 15 min after the re-addition of Ca^{2+}. After 5 h of Ca^{2+} re-addition, Trio–VE-cadherin interactions had been restored to basal levels (Fig. 5B). The phenotypic reassembly of cell–cell junctions after treatment with EGTA was visible 60 min after re-addition of Ca^{2+}. However, in Trio-deficient cells, the recovery of junctions was still largely impaired at these time points (supplementary material Fig. S2C).

Additionally, we used thrombin to induce junction remodeling and to study the regulation of the Trio–VE-cadherin interaction. Analysis of the immunoprecipitation of Trio showed that 30 min after stimulation with thrombin, when thrombin-induced cell–cell junction disruption and resistance drop were maximal (Fig. 2B), Trio binding to VE-cadherin was reduced compared with that in untreated cells. However, the Trio–VE-cadherin interaction significantly increased during the recovery phase – i.e. when cell–cell junctions are re-assembled and the resistance is restored (Fig. 5C and Fig. 2B). The Trio–VE-cadherin interaction was also reduced after stimulation with the permeability factor VEGF (supplementary material Fig. S2D). Taken together, these experiments show that Trio dynamically associates with the VE-cadherin complex primarily at nascent cell–cell contacts.

Trio controls junction-associated actin organization

To examine the mechanism of how Trio controls endothelial cell–cell junction integrity, we next studied the effect of silencing Trio on the organization of the VE-cadherin complex and the actin cytoskeleton in more detail. Loss of cell–cell junction integrity in Trio-deficient endothelial cells did not result from changes in the expression levels of VE-cadherin, α-catenin, β-catenin, γ-catenin and p120-catenin or other junction adhesion molecules (supplementary material Fig. S2E). Also, by immunoprecipitating VE-cadherin from lysates, no changes were found in the composition of the VE-cadherin–catenin complex in Trio-deficient cells compared with controls (supplementary material Fig. S2F). Interestingly, overexpression of TrioN induced strong

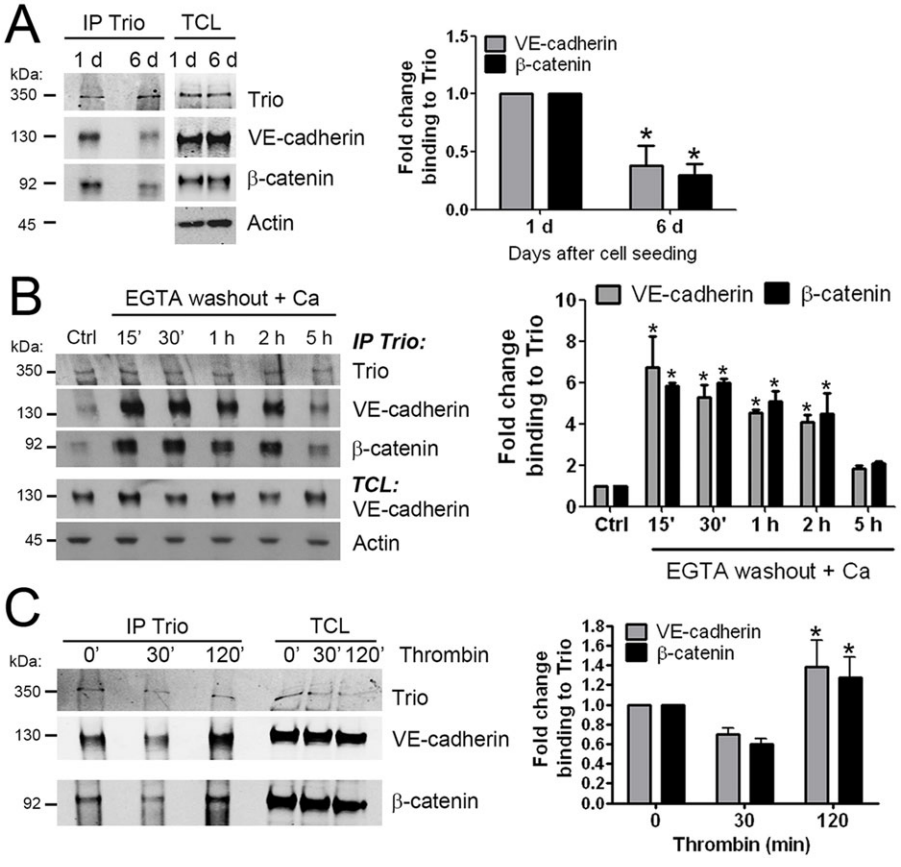

Fig. 5. Dynamic interaction of Trio–VE-cadherin. (A) Endothelial cells at different confluences (days after seeding are indicated above) were lysed and subjected to immunoprecipitation (IP) of Trio. Association of VE-cadherin and β-catenin with Trio was determined by western blotting. Quantification is shown in the right panel. TCL, total cell lysate. (B) Cells that had been cultured for 6 days, reaching full confluency, were subjected to Ca^{2+} switch – treatment with EGTA treatment to chelate extracellular Ca^{2+} leading to cell–cell junction disruption, followed by EGTA washout and Ca^{2+} re-addition resulting in junction reassembly. Endothelial cells were lysed at the indicated times after Ca^{2+} re-addition and Trio was immunoprecipitated. Quantification is shown in right panel and shows fold change in binding of Trio to VE-cadherin after treatment with EGTA compared with Trio–VE-cadherin binding under control conditions. (C) Endothelial cells were grown to confluence, stimulated with thrombin for 30 or 120 min, reflecting the time of cell–cell junction disassembly and reassembly, respectively. Cells were lysed and subjected to Trio immunoprecipitation. Association of VE-cadherin and β-catenin with Trio was determined by western blotting. Quantification is shown in the right panel and shows fold change in binding of Trio to VE-cadherin after thrombin treatment compared with Trio–VE-cadherin binding under control conditions. All experiments are performed at least three times. Data are mean±s.e.m. *P<0.05. Ca, Ca^{2+}.

Journal of Cell Science

Journal of Cell Science (2015) 128, 3041-3054 doi:10.1242/jcs.168674

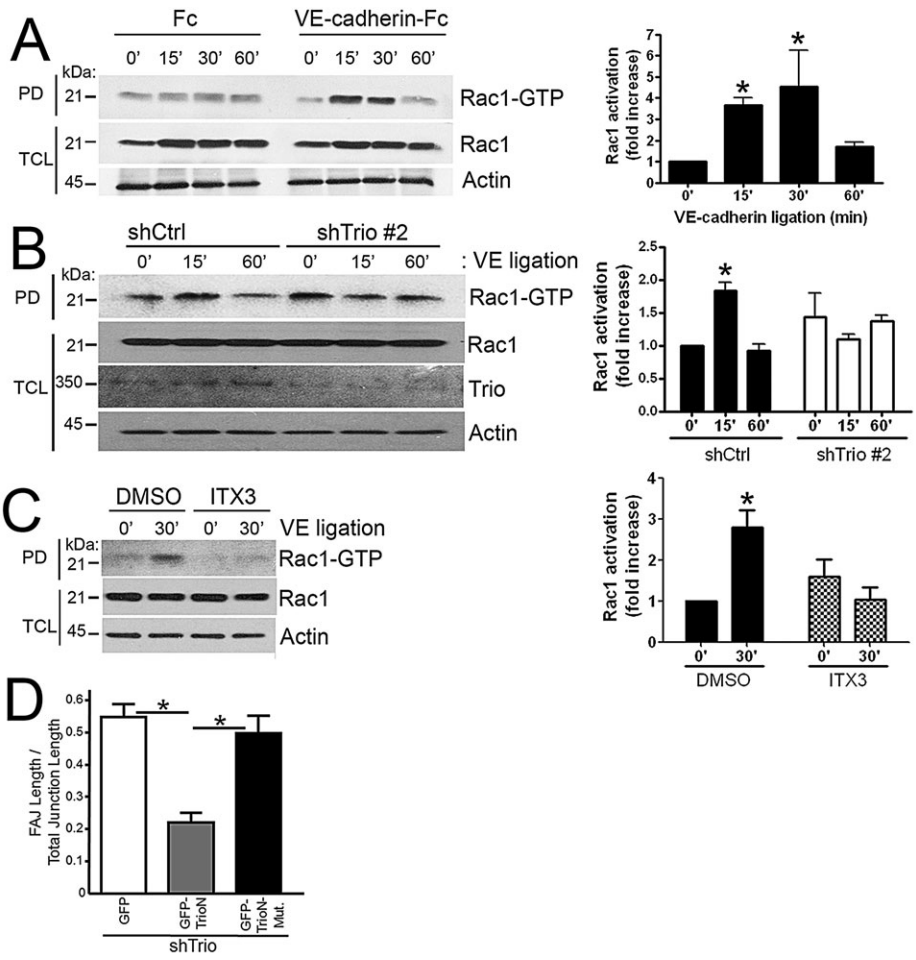

Fig. 6. VE-cadherin-induced Rac1 activation depends on Trio. (A–D) VE-cadherin-ectodomain-Fc- or Fc-coated magnetic beads were added to an endothelial monolayer to induce VE-cadherin ligation. (A) Rac1 activation increases 15–30 min after adding VE-cadherin-coated beads, as analyzed using a CRIB-peptide pulldown (PD) assay. Right panel shows the quantification. (B) Endothelial cells were transduced with a control shRNA (shCtrl) or a shRNA against Trio (shTrio #2). VE-cadherin ligation did not increase Rac1 activation in Trio-deficient cells. Right panel shows quantification. Time (min) after addition of VE-cadherin-ectodomain-Fc-coated beads is shown. (C) VE-cadherin ligation was induced in endothelial cells treated with DMSO or the Trio-GEF1 inhibitor ITX3. Treatment with ITX3 blocks VE-cadherin ligation-induced Rac1 activation. Right panel shows quantification. Time (min) after addition of VE-cadherin-ectodomain-Fc-coated beads is shown. (D) Trio-deficient endothelial cells (shTrio) were transfected with GFP, wild-type GFP–TrioN or a mutant GFP–TrioN construct comprising two mutations (N1406A/D1407A, GFP–TrioN-Mut), and the length of the FAJs was quantified as described previously. For each condition, 25 cells were analyzed. All experiments were performed at least three times independently. Data are mean±s.e.m. *P<0.05.

cortical actin bundles at VE-cadherin-based junction regions (Fig. 3A; supplementary material Fig. S3A). Because the function of VE-cadherin is known to be strongly influenced by re-arrangements of the actin cytoskeleton (Oldenburg and de Rooij, 2014), we next examined whether Trio controls junctional actin organization through the small GTPase Rac1.

VE-cadherin ligation activates Rac1 through Trio

In epithelial cells, replacement of radial actin bundles by a peri-junctional actin belt has been proposed to be controlled by cadherins, the homophilic ligation of which can directly recruit and activate actin regulators (Cavey and Lecuit, 2009). Therefore, we studied whether VE-cadherin homophilic ligation induces Trio-dependent Rac1 activation. To biochemically analyze a defined number of nascent VE-cadherin-mediated adhesive contacts, endothelial cells were incubated with magnetic beads that had been coated with the ecto-domain of VE-cadherin. VE-cadherin-coated beads specifically ligate endogenous VE-cadherin complexes (supplementary material Fig. S3B). Interestingly, Rac1 activation was increased 15–30 min following VE-cadherin ligation, after which activation levels declined (Fig. 6A). By contrast, VE-cadherin ligation reduced the activation of both RhoG and RhoA (supplementary material Fig. S3C,D). We next studied whether Trio underlies VE-cadherin-ligation-induced Rac1 activation. Although basal levels of Rac1 activity were increased in Trio-depleted cells compared with that of controls, silencing of Trio blocked the increase in Rac1 activity that was observed after VE-cadherin ligation (Fig. 6B). We confirmed this with a different shRNA that targeted Trio expression (supplementary material Fig. S3E). Additionally, we observed that inhibition of GEF1 by ITX3 blocked VE-cadherin-ligation-dependent Rac1 activation (Fig. 6C).

To show the functional involvement of the GEF1 domain in junction regulation, we expressed TrioN in Trio-deficient endothelial cells and studied the total lengths of the FAJs (Fig. 6D). To check whether the activity of the GEF1 domain is required, we induced two point mutations (N1406A/D1407A) in GEF1, resulting in a catalytically dead protein that was unable to activate Rac1 (supplementary material Fig. S3F). Expression of the catalytically dead mutant did not reduce FAJ length in Trio-deficient cells (Fig. 6D). Additional experiments showed that TrioN-induced linearization of cell–cell junctions is independent of RhoG (supplementary material Fig. S3G). Collectively, these data indicate that Trio is involved in Rac1 activation upon VE-cadherin ligation and that it mediates linearization of cell–cell junctions.

We next studied the spatial and temporal activation of Rac1 during endothelial cell–cell junction formation by using a novel Rac1 sensor called the dimerization-optimized reporter for activation (DORA)-based Rac1-sensor (supplementary material Fig. S4A). We first characterized the sensor for local Rac1 activation in random migrating endothelial cells (supplementary material Fig. S4B, Movie 5), as well as in epidermal growth factor (EGF)-treated HeLa cells (supplementary material Fig. S4C,D). Additionally, we measured spatial and temporal Rac1 inactivation and activation upon treatment with thrombin in endothelial cells (supplementary material Fig. S4E, Movie 5). Moreover, we

Journal of Cell Science

Journal of Cell Science (2015) 128, 3041-3054 doi:10.1242/jcs.168674

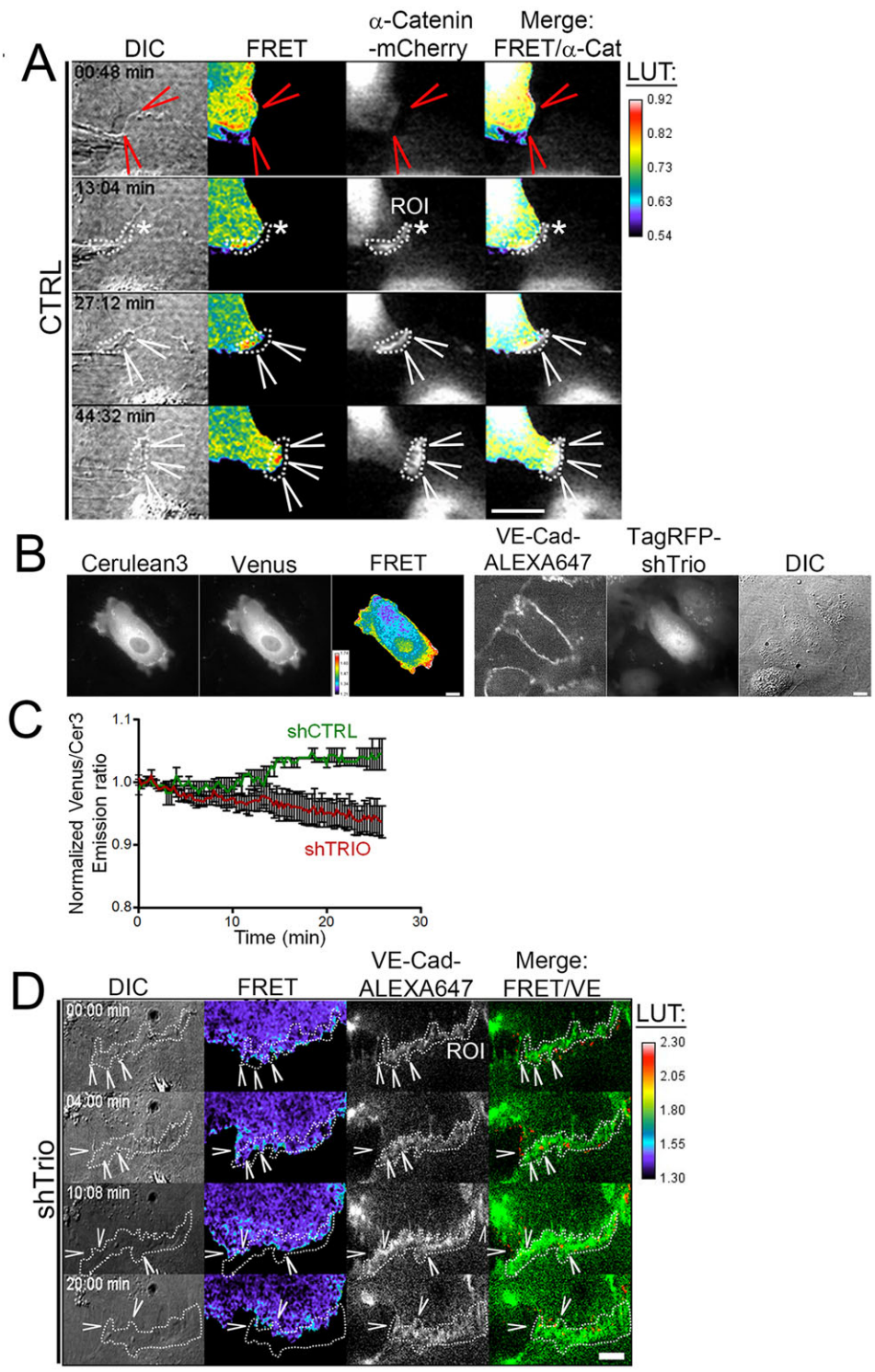

Fig. 7. Spatio-temporal Rac1 activity. (A) Endothelial cells were transfected with the DORA Rac1 biosensor and α-catenin–mCherry to mark cell–cell junctions. Panels show differential interference contrast (DIC) microscopy images, ratiometric images with warm colors as increased FRET (Venus and Cerulean3) signals [see look-up table (LUT) on the right], α-catenin–mCherry and the merge with FRET in red, and the merge with α-catenin–mCherry in white. Arrowheads show colocalization of local active Rac1 with α-catenin. Asterisks show formation of nascent cell–cell junctions. The times after beginning observation are shown. (B) Trio-deficient endothelial cells are marked by TagRFP (TagRFP-shTrio); the junction region is marked by the VE-cadherin-AlexaFluor-647 antibody, because the red channel is used to detect TagRFP. All fluorescent signals were recorded in real time. (C) Quantification of the ratiometric changes at regions of nascent cell–cell junctions, marked by α-catenin or VE-cadherin (dotted line in panels A and D), show an increased FRET signal after approximately 15 min in shCTRL but not in Trio-deficient endothelial cells. The graph shows data that is representative of three independent experiments. Data are mean± s.e.m. (D) Trio-deficient endothelial cells (marked by TagRFP–shTrio) show no increase in FRET signal at sites of newly formed cell–cell junctions, marked by the VE-cadherin-AlexaFluor-647 antibody (arrowheads). Note that the basal FRET signals (LUT) are higher in Trio-deficient cells than in control cells (compare with LUT in A), in line with the biochemical data. Scale bars: 10 µm (A,B); 5 µm (D).

performed fluorescence-lifetime imaging microscopy (FLIM) measurements in cells that expressed the wild-type Rac sensor or the constitutively active (Q61L) mutant sensor, showing a reduced lifetime of the Q61L mutant compared with that of the wild-type version (2.4 vs 2.9 ns, respectively) (supplementary material Fig. S4F). Importantly, the dominant-negative Rac1 sensor did not show any activity upon the random migration of endothelial cells (supplementary material Fig. S4G). For more detailed text, see supplementary material Fig. S4. These experiments showed that the DORA Rac1 sensor can be used to efficiently measure spatio-temporal activation of Rac1 upon cell–cell junction assembly.

Endothelial cells were transfected with the DORA Rac1 sensor and α-catenin–mCherry to visualize the VE-cadherin complex. We monitored FRET during the assembly and disassembly cycle of forming junctions. At the initial stage of junction assembly, marked by α-catenin–mCherry, no FRET signal was detected (Fig. 7A; supplementary material Movie 6). However, after approximately 15 min, increased FRET at α-catenin-selected regions of interest (ROI) was detected, showing local Rac1 activity at cell–cell

Journal of Cell Science (2015) 128, 3041-3054 doi:10.1242/jcs.168674

junction regions (Fig. 7A,C; supplementary material Movie 6). These data indicate that formation of nascent cell–cell junctions triggers local activation of Rac1. To investigate whether Trio is involved in the local activation of Rac1 at nascent cell–cell junctions, we analyzed endothelial cells expressing TagRFP–Trio shRNAs and the DORA-Rac1 biosensor. To properly discriminate cell–cell junctions, we additionally live-labeled with an AlexaFluor-647-conjugated antibody against VE-cadherin (Fig. 7B). We have previously shown that this antibody does not interfere with the dynamics of VE-cadherin or the barrier function (Kroon et al., 2014). Using this setup, we observed that junctions in Trio-deficient endothelial cells rapidly dis- and re-assemble, as shown previously. Interestingly, no increase in local Rac1 activity was measured at VE-cadherin-based junctions in Trio-deficient cells (Fig. 7D; supplementary material Movie 7). Quantification of the emission ratio of the FRET showed a lack of Rac1 activity at selected cell–cell contact regions (ROI), marked by VE-cadherin, in Trio-deficient cells (Fig. 7C). Interestingly, we observed localized Rac1 activity at the edge of non-junctional membrane protrusions in Trio-deficient cells, indicating that Rac1-mediated induction of protrusions is not itself regulated through Trio (supplementary material Fig. S4G, Movie 8). However, in line with the previous experiment, at sites of junction assembly, marked by VE-cadherin, no increase in FRET was detected (supplementary material Fig. S4G, Movie 8). Taken together, these data show that Trio controls spatial and temporal activation of Rac1 at sites of newly formed VE-cadherin-based junctions.

DISCUSSION

Here, we show that Trio regulates stabilization of nascent, VE-cadherin-based cell–cell adherens junctions to maintain endothelial barrier properties. Mechanistically, we show that VE-cadherin ligation recruits Trio and that the clusters directly bind to Trio, triggering spatio-temporal activation of the small GTPase Rac1, followed by stabilization of endothelial adherens junctions.

The process of adherens junction formation can be subdivided into distinct stages – first, membrane protrusions generate initial contacts; second, cadherin molecules engage in homophilic interactions and form clusters; and third, homophilic ligation of cadherins triggers actin cytoskeleton rearrangements, driving expansion and stabilization of the cadherin adhesive interface (Cavey and Lecuit, 2009). Rac1 activity has been shown to be involved in several of these stages of adherens junction formation, but also in their dissociation (reviewed in Spindler et al., 2010). These apparently contradictory data underscore the importance of addressing spatial and temporal differences in Rac1 activity, and of understanding the involvement of specific GEF–GTPase-effector complexes. We propose that Trio activity is particularly crucial during the abovementioned third stage of the adherens junction formation process. This is based on our observation that local Rac1 activity at adherens junctions was rapidly increased in a Trio-dependent manner during nascent contact formation, as assessed using a novel FRET-based Rac1 biosensor. Moreover, homophilic ligation of VE-cadherin, triggered by VE-cadherin-coated beads, stimulated rapid and transient Trio-dependent Rac1 activation. In line with this, adherens junctions in Trio-deficient cells remained unstable and underwent continuous disassembly and reassembly. Importantly, Trio-deficiency did not prevent Rac1-induced membrane protrusive activity or the formation of initial cell–cell contacts. Thus, prior to stabilization of the nascent cell–cell contact that is induced by local signaling through the VE-cadherin–Trio–Rac1 axis, other Rac-GEFs are likely to contribute to the promotion of the formation of initial cell–cell contacts. For example Tiam-1, which is well recognized for its role in promoting epithelial cell–cell adhesion (Hordijk et al., 1997), has also been suggested to have a role in controlling endothelial cell–cell junctions; re-introduction of VE-cadherin in VE-cadherin-null cells induces Rac1 activation and recruits Tiam-1 to cell–cell junctions (Birukova et al., 2012; Lampugnani et al., 2002). Conversely, Tiam-1 is reported to be required for the increased permeability that is induced by platelet-activating factor (Knezevic et al., 2009). Clearly, further study is needed to unravel how Trio can act in concert with other Rac-GEFs, such as Tiam-1, Vav2 (Gavard and Gutkind, 2006) and PRex1 (Naikawadi et al., 2012), to control endothelial adherens junctions under resting or inflammatory conditions.

To our knowledge, Trio is the first example of a GEF binding to the cytoplasmic domain of VE-cadherin. Other GEFs, such as Tiam1, Syx and TEM4, have been shown to localize at endothelial cell–cell junctions or to co-immunoprecipitate with one of the VE-cadherin complex members, but no *in vitro* interaction studies using peptides or GST–tagged proteins have been performed so far (Di Lorenzo et al., 2013; Lampugnani et al., 2002; Ngok et al., 2012, 2013). We found that Trio had a particular affinity for the pool of VE-cadherin at (re-)assembling junctions, enabling temporally coordinated Rac1 activation. Although we could show that Trio binds to a region in VE-cadherin that is proximal to the β-catenin-binding domain, our experiments indicate that Trio does not seem to compete with β-catenin for binding to VE-cadherin but that it might in fact form a ternary complex. Previously, Trio has been reported to biochemically co-precipitate with M-cadherin, cadherin-11 and E-cadherin (Backer et al., 2007; Charrasse et al., 2007; Kashef et al., 2009; Li et al., 2012; Yano et al., 2011). In the latter study, the activity of Trio at E-cadherin-based epithelial cell–cell junctions is described as down regulating E-cadherin expression levels by activating a transcriptional repressor of E-cadherin (Yano et al., 2011). By contrast, our data show that the total protein levels of VE-cadherin and N-cadherin are unaltered in Trio-deficient endothelial cells. Thus, Trio has distinct regulatory roles at adherens junctions depending on the cadherin and cell type involved. Elucidating the mechanism of how Trio is activated and recruited to the VE-cadherin complex will be exciting goals for future research.

Our finding that silencing of Trio impairs endothelial barrier recovery in response to thrombin supports our hypothesis that Trio activity is not only crucial for *de novo* assembly of adherens junctions, but also for reassembly of adherens junctions following inflammatory remodeling of the vascular endothelium. In addition, even apparently stable endothelial monolayers display ongoing remodeling of cell–cell junctions, and Rac1 activation in confluent endothelial monolayers has been suggested to reflect such local remodeling (Braga and Yap, 2005). Our finding that Trio-induced Rac1 activity contributes to the maintenance of the endothelial barrier might therefore reflect, on a smaller scale, the requirement of Trio for the reassembly of cell–cell contacts. During remodeling of endothelial adherens junctions, the morphologies of cell–cell junctions switch between linear adherens junctions, which are in parallel to cortical actin bundles, and focal adherens junctions, which are connected to radial actin bundles (Huveneers et al., 2012). We found that Trio contributes to the transition of radial actin bundles into cortical actin bundles, promoting the formation of stable linear adherens junctions. It has been suggested that this transition of junctional actin organization takes place very shortly after the initial clustering of cadherins (Cavey and Lecuit, 2009). This is in full accordance with our observations when measuring active Rac1 in real-time. We observed that Rac1 is activated several

Journal of Cell Science

Journal of Cell Science (2015) 128, 3041-3054 doi:10.1242/jcs.168674

minutes after the initial cell–cell junctions are formed, and although it is well known that Rac1 localizes at *de novo* adhesion sites and promotes lamellipodia formation through actin remodeling (Yamada and Nelson, 2007; Yamazaki et al., 2007; Zhang et al., 2005), further study is required to elucidate the detailed mechanism of how Trio-induced Rac1 activity triggers actin cytoskeletal rearrangements upon VE-cadherin ligation. An interesting side observation is that Trio-deficient cells showed a higher basal level of Rac1 activity, as well as increased migration. One explanation for increased Rac1 activation might be that the unstable cell–cell junctions in Trio-deficient cells trigger the release of a different Rac1 pool that becomes activated. This could also explain the increased spread surface area that was observed for Trio-deficient cells. In other cell types, cadherin ligation has been shown to recruit and activate actin regulators, including Arp2/3 (Kovacs et al., 2002; Verma et al., 2004), cortactin (Helwani et al., 2004), N-WASP (Ivanov et al., 2005) and formin1 (Kobielak et al., 2004) (for review, see Bershadsky, 2004; Yap and Kovacs, 2003). Some of these factors that promote branched actin polymerization have been found to be relatively depleted from older, more stable regions of epithelial cell–cell contacts (Helwani et al., 2004; Yamada and Nelson, 2007). Although there are notable differences between epithelial and endothelial cell–cell contacts with respect to the organization of the junction-associated actin cytoskeleton, similar actin regulators could be involved in VE-cadherin-based strengthening of adherens junctions.

In conclusion, Trio regulates the spatial and temporal activation of Rac1 to drive VE-cadherin-based reassembly of adherens junctions, not only after endothelial cell barrier disruption that has been induced by inflammatory agents such as thrombin, but also for *de novo* assembly of adherens junctions. Eventually, enhancing the VE-cadherin–Trio interaction could be considered as a novel potential therapeutic approach that might serve to counteract vascular leakage and/or inflammation.

MATERIALS AND METHODS

Antibodies

Monoclonal antibodies (mAb) to β-catenin, p120-catenin, γ-catenin, Cdc42 (clone 44), Rac1, VE-cadherin (clone 75; used at 6.25 µg/ml) and an AlexaFluor-647-conjugated antibody against VE-cadherin (clone 7H1) were purchased from BD Transduction Laboratories (Amsterdam, The Netherlands). mAbs to VE-cadherin (clone F8), RhoA and polyclonal Abs (pAb) to β-catenin, α-catenin and Trio (clone D-20) were purchased from Santa Cruz Biotechnology (Heidelberg, Germany). An mAb against Trio was from Abnova (Heidelberg, Germany). VE-cadherin mAb clone 7H1 was from Pharmingen (San Diego, CA), VE-cadherin clone BV6 and RhoG mAbs were from Millipore (Amsterdam, The Netherlands). pAb to VE-cadherin was from Cayman (Ann Arbor, MI). mAbs to α-tubulin (DM1A), actin (clone AC-40), and hemagglutinin (HA) were purchased from Sigma (Zwijndrecht, The Netherlands). pAb to VEGFR2 and pAb to mouse PECAM-1 were from R&D (Abingdon, UK). An antibody against PECAM-1 (CD31, clone 12F11) was from Sanquin (Amsterdam, The Netherlands). mAb against GFP (clone JL-8), secondary goat-anti-rabbit IR 680, goat-anti-mouse IR 800 and donkey anti-goat IR 800 antibodies were purchased from Licor Westburg (Leusden, The Netherlands). Antibodies to N-cadherin, Myc, ZO-1 (clone A12), secondary AlexaFluor-labeled Abs and AlexaFluor-633-conjugated phalloidin and phalloidin–Texas-Red were from Invitrogen (Breda, The Netherlands). Secondary horseradish peroxidase (HRP)-conjugated goat-anti-mouse, swine-anti-rabbit and rabbit-anti-goat antibodies were purchased from Dako (Heverlee, Belgium).

Cell culture, treatments and transfections

HUVECs were purchased from Lonza and cultured on fibronectin-coated dishes in EGM-2 medium, which was supplemented with singlequots (Lonza, Verviers, Belgium). HUVECs were cultured until passage 7. HEK293T, Cos7 and CHO cells were maintained in Iscove's modified Dulbecco's medium (IMDM) (BioWhittaker, Verviers, Belgium) containing 10% (v/v) heat-inactivated fetal calf serum (Invitrogen, Breda, The Netherlands), 300 mg/ml L-glutamine, 100 U/ml penicillin–streptomycin. Cells were cultured at 37°C under 5% CO_2. Cells were pretreated for 20 h at 37°C with 100 µM ITX3, purchased from ChemBridge (San Diego, CA) (Bouquier et al., 2009). Cells were pretreated for 1 h with 12.5 µM EHT-1864 (Sigma) (Onesto et al., 2008). Cells were transfected according to the manufacturer's protocol with Trans IT-LT1 reagent (Myrus, Madison, WI) or electroporation (1 pulse, 1350 V, 30 ms) (Invitrogen). GFP-tagged VE-cadherin constructs (VEΔβΔIMD–GFP, VEΔC-α–GFP and VEΔC-αΔN–GFP) were a kind gift from Dr Naoki Mochizuki (National Cardiovascular Center Research Institute, Osaka, Japan) (Noda et al., 2010). Adenovirus Trio and VE-cadherin–GFP constructs were generated as described previously (Allingham et al., 2007; van Rijssel J. et al., 2012b). One day after adenoviral infection, medium was replaced; 2–3 days after infection, cells were used for assays. α-Catenin–mCherry and shRNA constructs (Sigma Mission library) targeting Trio (shTrio#1, TRC_10561; shTrio#2, TRC_873), VE-cadherin (TRC_54090) or a non-targeting shCtrl (shC002) were packaged into lentivirus in HEK293T cells by means of third generation lentiviral packaging plasmids. Lentivirus-containing supernatant was harvested on day 2 and 3 after transfection. Lentivirus was concentrated by centrifugation at 20,000 ***g*** for 2 h. Target cells were infected and, 3 days after the addition of virus, cells were used for assays.

Confocal laser scanning microscopy

Cells were cultured on fibronectin-coated glass coverslips and transfected/stimulated as indicated. After treatment, cells were washed with ice-cold PBS, containing 1 mM $CaCl_2$ and 0.5 mM $MgCl_2$, and fixed in 4% (v/v) formaldehyde for 10 min. After fixation, cells were permeabilized in PBS with 0.2% (v/v) Triton X-100 for 10 min followed by a blocking step in PBS with 2% (w/v) BSA and incubated with primary and secondary antibodies, and after each step, cells were washed with PBS. Fluorescence imaging was performed with a confocal laser scanning microscope (LSM510/Meta; Carl Zeiss MicroImaging) using a 63× NA1.40 or a 40× NA1.30 oil lens. The pixel area was determined as described previously (Timmerman et al., 2012).

DORA Rac1-sensor constructs

Development of the DORA single-chain Rac1 biosensor

Dimeric Cerulean3 coupled to the Rac1 effector p21-activated protein kinase 1 (PAK1) was linked through a ribosomal protein-based linker (L9H) with circular-permutated Venus coupled to Rac1. The DORA Rac1 sequence within a pTriEx-HisMyc backbone was dCer3(G229)-KpnI-GS-PAK(I75-K118)-L9H-L9H-BamHI-GS-dcpVen-NheI-Rac-WT-HindIII. The DORA Rac1 mutant PAK biosensor sequence within a pTriEx-HisMyc backbone was dCer3(G229)-KpnI-GS-PAK(I75-K118, H83,86D)-L9H-L9H-BamHI-GS-dcpVen-NheI-Rac-WT-HindIII. The histidine residues (H) at positions 83 and 86 in the PAK domain of the Rac1 control biosensor were substituted for an aspartic acid residue (D) and used as a negative control.

FRET measurements

Rac1 activity was measured in living cells by monitoring yellow fluorescent protein (YFP) FRET over donor cyan fluorescent protein (CFP) intensities. A Zeiss Observer Z1 microscope with 40× NA1.3 oil immersion objective, a HXP 120 V excitation light source, a Chroma 510 DCSP dichroic splitter, and two Hamamatsu ORCA-R2 digital CCD cameras for simultaneous monitoring of Cerulean3 and Venus emissions were used. Image acquisition was performed using Zeiss-Zen 2011 microscope software. Offline ratio analysis between Cerulean3 and Venus images were processed using MBF ImageJ collection. Raw Cerulean3 and Venus images were background (BG)-corrected using the plug-in 'ROI, BG subtraction from ROI'. Cerulean3 and Venus stacks were aligned using the registration plug-in 'Registration, MultiStackReg'. A smooth filter was applied to both image

Journal of Cell Science (2015) 128, 3041-3054 doi:10.1242/jcs.168674

stacks to improve image quality by reducing noise. Image stacks were converted to a 32-bit image format and a threshold was applied exclusively to the Venus image stack, converting the background pixels to 'not a number' (NaN), allowing elimination of artifacts in ratio image stemming from the background noise. Finally, the Venus:Cer3 ratio was calculated using the plug-in 'Ratio Plus', and a custom look-up table was applied to generate a heatmap. MultiStackReg and Ratio Plus are available through the ImageJ website (http://rsb.info.nih.gov/ij/plugins/index.html). To label cell–cell junctions, we used α-catenin–mCherry in the control cells. In TagRFP Trio-deficient cells, the red channel was in use. Therefore, an antibody against VE-cadherin that had been directly labelled with a fluorophore (VE-cadherin-AlexaFluor-647, Millipore). FLIM analysis was performed using a dedicated Zeiss Axiovert wide-field microscope that had been equipped with instruments to perform frequency-domain FLIM imaging and a 63× (Plan Apochromat NA1.4 oil) objective.

Immunoprecipitation and western blot analysis

Cells were washed twice with ice-cold PBS, containing 1 mM $CaCl_2$ and 0.5 mM $MgCl_2$, and lysed in cold NP-40 lysis buffer [25 mM Tris, 100 mM NaCL, 10 mM $MgCl_2$, 10% (v/v) glycerol and 1% (v/v) Nonidet P-40, pH 7.4] supplemented with a phosphatase inhibitor cocktail (Sigma) and fresh protease-inhibitor-mixture tablets (Roche Applied Science). After 10 min, cell lysates were collected and centrifuged at 14,000 ***g*** for 10 min at 4°C. The supernatant was incubated with 0.5 µg of mAb to VE-cadherin (clone BV6, Millipore) or 2 µg goat pAb to Trio (clone D-20, Santa Cruz) and 50 µl of protein-G–Sepharose at 4°C with continuous mixing. In other experiments, biotinylated-peptides (1 µg/ml) together with streptavidin–agarose were used. Subsequently, beads were centrifuged at 5000 rpm for 20 s at 4°C, washed five times with NP-40 lysis buffer and boiled in SDS sample buffer containing 4% β-mercaptoethanol. Samples were analyzed by using SDS-PAGE. Proteins were transferred onto a 0.2 µm nitrocellulose membrane (Whatman, Dassel, Germany), subsequently blocked with 5% (w/v) milk powder in Tris-buffered saline with Tween20 (TBST). The nitrocellulose membrane was incubated with specific primary antibodies overnight at 4°C, followed by incubation with secondary HRP-labeled antibodies for 1 h at room temperature. Between the incubation steps, blots were washed with TBST. Staining was visualized with an enhanced chemiluminescence (ECL) detection system (ThermoScientific, Amsterdam, The Netherlands). Alternatively, blots were incubated with IR-680- or IR-800-dye-conjugated secondary antibodies. The infrared signal was detected and analyzed with the Odyssey infrared detection system (Li-cor Westburg).

GTPase activity assays

Cells were lysed in 50 mM Tris, pH 7.4, 0.5 mM $MgCl_2$, 500 mM NaCl, 1% (v/v) Triton X-100, 0.5% (w/v) deoxycholic acid (DOC) and 0.1% (w/v) SDS supplemented with protease inhibitors. Subsequently, lysates were cleared at 10,000 rpm for 10 min. GTP-bound Rac1 and Cdc42 were isolated by rotating supernatants for 30 min with 30 µg of a biotinylated PAK1-CRIB peptide, that had been coupled to streptavidin agarose (Price et al., 2003). GTP-bound RhoG was isolated by rotating supernatants for 30 min with 60 µg of GST–ELMO, pre-coupled to glutathione Sepharose beads (GE Healthcare, Zeist, The Netherlands) (van Buul et al., 2007; Wittchen and Burridge, 2008). Beads were washed five times in 50 mM Tris, pH 7.4, 0.5 mM MgCl2, 150 mM NaCl, 1% (v/v) Triton X-100 and boiled in SDS-sample buffer containing 4% β-mercaptoethanol. Samples were analyzed by using SDS-PAGE as described above. RhoA activation was measured using a G-LISA kit, according to the manufacturer's protocol (Cytoskeleton, Denver, CO).

VE-cadherin ectodomain-Fc-coated beads

Freestyle HEK cells were transfected with pcDNA-VE-Cad-Ect-Fc-His and pcDNA-Fc-His using 293Fectin. After 4 days, VE-cadherin-Fc (VE-Fc) protein that had been secreted into the medium was collected and centrifuged to remove cell debris. His-tagged proteins were purified using a Chelating Sepharose column (GE Healthcare) charged with nickel. VE-Fc or Fc protein was eluted with 250 mM imidazole after which the buffer was exchanged into PBS containing 1 mM $CaCl_2$ by using dialysis. Dynabeads (Invitrogen) were incubated with 2 µg of VE-Fc or Fc diluted in PBS containing 2 mM EDTA and 0.1% (w/v) BSA for 45 min under constant head-over-head rotation at 4°C. Dynabeads were washed and added to the cells for the indicated time to allow homophilic VE-cadherin engagement. Cells were washed twice with ice-cold PBS, containing 1 mM $CaCl_2$ and 0.5 mM $MgCl_2$, and lysed in cold NP-40 lysis buffer. Subsequently a CRIB peptide-based pull-down was performed (see section GTPase activity assays) or VE-Fc-and Fc-coated Dynabeads were isolated using a magnetic holder, and the interacting proteins were studied. Dynabeads were washed twice with RIPA buffer, three times with NP40-lysis buffer and were then resuspended in SDS-PAGE sample buffer.

Electric cell-substrate impedance sensing (ECIS)

Monolayer integrity was determined by measuring the electrical resistance using ECIS. Electrode-arrays (8W10E; IBIDI, Planegg, Germany) were treated with 10 mM L-cysteine (Sigma) for 15 min at 37°C and subsequently coated with 10 µg/ml fibronectin (Sigma) in 0.9% NaCl for 1 h at 37°C. Cells were seeded at 100,000 cells per well (0.8 cm^2) and grown to confluence. Electrical resistance was continuously measured at 37°C under 5% CO_2 using ECIS model 9600 (Applied BioPhysics, New York, MA). Permeability was measured using Transwell filters with fibronectin-coated 0.1 µm pore size filters. Fluorescently labeled 3- or 10-kDa dextran was added to the upper compartment, and 5 h later the fluorescence in the lower compartment was measured using a fluorimeter.

VE-cadherin peptides

Peptides were synthesized corresponding to the intracellular sequence for VE-cadherin as indicated. Scrambled peptides were synthesized as negative controls with the lowest Needleman-wunsch alignment score and highest Levenshtien distance to original sequence. VE-cadherin peptide no. 1 sequence – GAHGGPGEMAAMIEVKKDEADHDGDGPPYDTLH IYGYEG. VE-cadherin peptide no. 2 sequence – TLHIYGYEGSESIAESLSSLGTDSSDSDVDYDFLNDWGP. Scrambled peptide sequence – SLEDISLEAYSGHYSEGTSGDDVSPDFSNDLSLGDTWDY. Protein-transduction domain (PTD) sequence – YARAAARQARA. Glycine was used as a linker. All peptides were biotinylated at the N-terminus. Pull-down assays were performed using streptavidin-coated magnetic beads.

GST pull-down assay

The different constructs of GST-tagged Trio spectrin repeats (i.e. of spectrin repeats 1 and 2 (1–2); 1,2,3 and 4 (1–4); 5 and 6 (5–6); as well as 5,6,7 and 8 (5–8) and of GST in pGEX6P1 vectors were expressed in *Escherichia coli* BL21 overnight at 18°C and purified according to the manufacturers' recommendations (Amersham Biosciences) using 50 mM Tris-HCl, pH 7.4, 500 mM NaCl, 10% glycerol, 5 mM β-mercaptoethanol, supplemented with protease inhibitor mixture tablets (Roche), as lysis buffer. GST-tagged Trio spectrin repeats or GST were eluted with 20 mM glutathione, 50 mM Tris-HCl, pH 7.4, 150 mM NaCl, 5% glycerol, 5 mM β-mercaptoethanol, from glutathione–Sepharose-4B beads and dialyzed twice using the same buffer but without glutathione. Proteins were aliquoted and stored at −80°C upon flash freezing in liquid nitrogen. To test for direct binding, the biotinylated peptides encoding the intracellular domains of VE-cadherin (as indicated) and scrambled peptide (CTRL) were coupled to streptavidin–agarose beads and incubated with purified GST-tagged Trio spectrin repeats (molar ratio 1:2, spectrin 1–2, spectrin 1–4, spectrin 5–6 or spectrin 5–8) in 50 mM Tris-HCl, pH 7.4, 150 mM NaCl, 10 mM $MgCl_2$, 5% glycerol, 5 mM β-mercaptoethanol for 1 h at 4°C under continuous mixing. Beads were washed five times and resuspended in SDS sample buffer. GST was used as control. The rate of activity was normalized by comparing the increase or decrease of GTPase activity to the expression levels of the GTPase in the total cell lysates.

Statistical analysis

Statistical comparisons between experimental groups were performed by using Student's *t*-test. A two-tailed *P*-value of ≤0.05 was considered significant.

Journal of Cell Science

Acknowledgements
We wish to thank Dr Giampietro Schiavo (London, UK) and Dr Veronika Neubrand (Granada, Spain) for the GST–spectrin-repeat constructs. We wish to thank Dr xxxxx Fukuhara and Dr Naoki Mochizuki (Osaka, Japan) for the kind gifts of the VE-cadherin mutants. GFP–TrioFL was a kind gift from Anne Debant and Philippe Fort (both at Macromolecular Biochemistry Research Center, Montpellier, France). Myc-TrioFL was a kind gift from Betty Eipper, University of Connecticut, Farmington, CT. We also wish to thank Anna E. Daniel for providing data. We sincerely thank Professor Dr Peter Hordijk for critically reading the manuscript. We wish to thank Dr Louis Hodgson (Department of Anatomy & Structural Biology, Albert Einstein University, New York, NY) for the Trio mutant constructs.

Competing interests
The authors declare no competing or financial interests.

Author contributions
I.T. and J.D.v.B. designed the study, performed and analyzed the experiments and wrote the paper. N.H., J.K., A.S., J.v.R. and M.H. performed the experiments. J.v.U. and J.G. performed and analyzed the characterization of the sensor experiments. T.W.J.G. supervised and analyzed the sensor characterization experiments. T.Y. and Y.W. generated and characterized the sensor. S.H. designed and analyzed the experiments, and wrote the paper.

Funding
This work is supported by a Landsteiner Foundation for Blood Transfusion Research (LSBR) fellowship [grant number 1028). J.D.v.B. is a Dekker fellow (DHF) [grant number 2005T039]. M.H. and A.S. were funded by a LSBR project grant [grant number 0903]. J.K. was supported by the DHF [grant number 2005T0391].

Supplementary material
Supplementary material available online at
http://jcs.biologists.org/lookup/suppl/doi:10.1242/jcs.168674/-/DC1

References

Allingham, M. J., van Buul, J. D. and Burridge, K. (2007). ICAM-1-mediated, Src- and Pyk2-dependent vascular endothelial cadherin tyrosine phosphorylation is required for leukocyte transendothelial migration. *J. Immunol.* **179**, 4053-4064.
Backer, S., Hidalgo-Sánchez, M., Offner, N., Portales-Casamar, E., Debant, A., Fort, P., Gauthier-Rouvière, C. and Bloch-Gallego, E. (2007). Trio controls the mature organization of neuronal clusters in the hindbrain. *J. Neurosci.* **27**, 10323-10332.
Bershadsky, A. (2004). Magic touch: how does cell–cell adhesion trigger actin assembly? *Trends Cell Biol.* **14**, 589-593.
Birukova, A. A., Tian, Y., Dubrovskyi, O., Zebda, N., Sarich, N., Tian, X., Wang, Y. and Birukov, K. G. (2012). VE-cadherin trans-interactions modulate Rac activation and enhancement of lung endothelial barrier by iloprost. *J. Cell Physiol.* **227**, 3405-3416.
Blangy, A., Vignal, E., Schmidt, S., Debant, A., Gauthier-Rouviere, C. and Fort, P. (2000). TrioGEF1 controls Rac- and Cdc42-dependent cell structures through the direct activation of rhoG. *J. Cell Sci.* **113**, 729-739.
Bouquier, N., Vignal, E., Charrasse, S., Weill, M., Schmidt, S., Léonetti, J.-P., Blangy, A. and Fort, P. (2009). A cell active chemical GEF inhibitor selectively targets the Trio/RhoG/Rac1 signaling pathway. *Chem. Biol.* **16**, 657-666.
Braga, V. M. M. and Yap, A. S. (2005). The challenges of abundance: epithelial junctions and small GTPase signalling. *Curr. Opin. Cell Biol.* **17**, 466-474.
Cavey, M. and Lecuit, T. (2009). Molecular bases of cell-cell junctions stability and dynamics. *Cold Spring Harb. Perspect. Biol.* **1**, a002998.
Charrasse, S., Comunale, F., Fortier, M., Portales-Casamar, E., Debant, A. and Gauthier-Rouvière, C. (2007). M-cadherin activates Rac1 GTPase through the Rho-GEF trio during myoblast fusion. *Mol. Biol. Cell* **18**, 1734-1743.
Corada, M., Liao, F., Lindgren, M., Lampugnani, M. G., Breviario, F., Frank, R., Muller, W. A., Hicklin, D. J., Bohlen, P. and Dejana, E. (2001). Monoclonal antibodies directed to different regions of vascular endothelial cadherin extracellular domain affect adhesion and clustering of the protein and modulate endothelial permeability. *Blood* **97**, 1679-1684.
Debant, A., Serra-Pages, C., Seipel, K., O'Brien, S., Tang, M., Park, S. H. and Streuli, M. (1996). The multidomain protein Trio binds the LAR transmembrane tyrosine phosphatase, contains a protein kinase domain, and has separate rac-specific and rho-specific guanine nucleotide exchange factor domains. *Proc. Natl. Acad. Sci. USA* **93**, 5466-5471.
Dejana, E. (2004). Endothelial cell–cell junctions: happy together. *Nat. Rev. Mol. Cell Biol.* **5**, 261-270.
Di Lorenzo, A., Lin, M. I., Murata, T., Landskroner-Eiger, S., Schleicher, M., Kothiya, M., Iwakiri, Y., Yu, J., Huang, P. L. and Sessa, W. C. (2013). eNOS-derived nitric oxide regulates endothelial barrier function through VE-cadherin and Rho GTPases. *J. Cell Sci.* **126**, 5541-5552.
Djinovic-Carugo, K., Gautel, M., Ylänne, J. and Young, P. (2002). The spectrin repeat: a structural platform for cytoskeletal protein assemblies. *FEBS Lett.* **513**, 119-123.
Gavard, J. and Gutkind, J. S. (2006). VEGF controls endothelial-cell permeability by promoting the beta-arrestin-dependent endocytosis of VE-cadherin. *Nat. Cell Biol.* **8**, 1223-1234.
Helwani, F. M., Kovacs, E. M., Paterson, A. D., Verma, S., Ali, R. G., Fanning, A. S., Weed, S. A. and Yap, A. S. (2004). Cortactin is necessary for E-cadherin-mediated contact formation and actin reorganization. *J. Cell Biol.* **164**, 899-910.
Hoelzle, M. K. and Svitkina, T. (2012). The cytoskeletal mechanisms of cell-cell junction formation in endothelial cells. *Mol. Biol. Cell* **23**, 310-323.
Hordijk, P. L., ten Klooster, J. P., van der Kammen, R. A., Michiels, F., Oomen, L. C. J. M. and Collard, J. G. (1997). Inhibition of invasion of epithelial cells by Tiam1-Rac signaling. Science **278**, 1464-1466.
Hultin, S., Zheng, Y., Mojallal, M., Vertuani, S., Gentili, C., Balland, M., Milloud, R., Belting, H.-G., Affolter, M., Helker, C. S. M. et al. (2014). AmotL2 links VE-cadherin to contractile actin fibres necessary for aortic lumen expansion. *Nat. Commun.* **5**, 3743.
Huveneers, S. and de Rooij, J. (2013). Mechanosensitive systems at the cadherin-F-actin interface. *J. Cell Sci.* **126**, 403-413.
Huveneers, S., Oldenburg, J., Spanjaard, E., van der Krogt, G., Grigoriev, I., Akhmanova, A., Rehmann, H. and de Rooij, J. (2012). Vinculin associates with endothelial VE-cadherin junctions to control force-dependent remodeling. *J. Cell Biol.* **196**, 641-652.
Ivanov, A. I., Hunt, D., Utech, M., Nusrat, A. and Parkos, C. A. (2005). Differential roles for actin polymerization and a myosin II motor in assembly of the epithelial apical junctional complex. *Mol. Biol. Cell* **16**, 2636-2650.
Kashef, J., Köhler, A., Kuriyama, S., Alfandari, D., Mayor, R. and Wedlich, D. (2009). Cadherin-11 regulates protrusive activity in Xenopus cranial neural crest cells upstream of Trio and the small GTPases. *Genes Dev.* **23**, 1393-1398.
Knezevic, I. I., Predescu, S. A., Neamu, R. F., Gorovoy, M. S., Knezevic, N. M., Easington, C., Malik, A. B. and Predescu, D. N. (2009). Tiam1 and Rac1 are required for platelet-activating factor-induced endothelial junctional disassembly and increase in vascular permeability. *J. Biol. Chem.* **284**, 5381-5394.
Kobielak, A., Pasolli, H. A. and Fuchs, E. (2004). Mammalian formin-1 participates in adherens junctions and polymerization of linear actin cables. *Nat. Cell Biol.* **6**, 21-30.
Kovacs, E. M., Goodwin, M., Ali, R. G., Paterson, A. D. and Yap, A. S. (2002). Cadherin-directed actin assembly: E-cadherin physically associates with the Arp2/3 complex to direct actin assembly in nascent adhesive contacts. *Curr. Biol.* **12**, 379-382
Kroon, J., Daniel, A. E., Hoogenboezem, M. and Van Buul, J. D. (2014). Real-time imaging of endothelial cell-cell junctions during neutrophil transmigration under physiological flow. *J. Vis. Exp.* **90**, e51766.
Lambert, J. M., Lambert, Q. T., Reuther, G. W., Malliri, A., Siderovski, D. P., Sondek, J., Collard, J. G. and Der, C. J. (2002). Tiam1 mediates Ras activation of Rac by a PI(3)K-independent mechanism. *Nat. Cell Biol.* **4**, 621-625.
Lampugnani, M. G., Resnati, M., Raiteri, M., Pigott, R., Pisacane, A., Houen, G., Ruco, L. P. and Dejana, E. (1992). A novel endothelial-specific membrane protein is a marker of cell-cell contacts. *J. Cell Biol.* **118**, 1511-1522.
Lampugnani, M. G., Zanetti, A., Breviario, F., Balconi, G., Orsenigo, F., Corada, M., Spagnuolo, R., Betson, M., Braga, V. and Dejana, E. (2002). VE-cadherin regulates endothelial actin activating Rac and increasing membrane association of Tiam. *Mol. Biol. Cell* **13**, 1175-1189.
Li, Y., Guo, Z., Chen, H., Dong, Z., Pan, Z. K., Ding, H., Su, S.-B. and Huang, S. (2012). HOXC8-dependent cadherin 11 expression facilitates breast cancer cell migration through Trio and Rac. *Genes Cancer* **2**, 880-888.
Naikawadi, R. P., Cheng, N., Vogel, S. M., Qian, F., Wu, D., Malik, A. B. and Ye, R. D. (2012). A Critical Role for Phosphatidylinositol (3,4,5)-Trisphosphate–Dependent Rac Exchanger 1 in Endothelial Junction Disruption and Vascular Hyperpermeability. *Circ. Res.* **111**, 1517-1527.
Navarro, P., Caveda, L., Breviario, F., Mândoteanu, I., Lampugnani, M. G. and Dejana, E. (1995). Catenin-dependent and -independent functions of vascular endothelial cadherin. *J. Biol. Chem.* **270**, 30965-30972.
Navarro, P., Ruco, L. and Dejana, E. (1998). Differential localization of VE- and N-cadherins in human endothelial cells: VE-cadherin competes with N-cadherin for junctional localization. *J. Cell Biol.* **140**, 1475-1484.
Ngok, S. P., Geyer, R., Liu, M., Kourtidis, A., Agrawal, S., Wu, C., Seerapu, H. R., Lewis-Tuffin, L. J., Moodie, K. L., Huveldt, D. et al. (2012). VEGF and Angiopoietin-1 exert opposing effects on cell junctions by regulating the Rho GEF Syx. *J. Cell Biol.* **199**, 1103-1115.
Ngok, S. P., Geyer, R., Kourtidis, A., Mitin, N., Feathers, R., Der, C. and Anastasiadis, P. Z. (2013). TEM4 is a junctional Rho GEF required for cell–cell adhesion, monolayer integrity and barrier function. *J. Cell Sci.* **126**, 3271-3277.
Noda, K., Zhang, J., Fukuhara, S., Kunimoto, S., Yoshimura, M. and Mochizuki, N. (2010). Vascular endothelial-cadherin stabilizes at cell-cell junctions by anchoring to circumferential actin bundles through alpha- and beta-catenins in cyclic AMP-Epac-Rap1 signal-activated endothelial cells. *Mol. Biol. Cell* **21**, 584-596.
Oldenburg, J. and de Rooij, J. (2014). Mechanical control of the endothelial barrier. *Cell Tissue Res.* **355**, 545-555.

Onesto, C., Shutes, A., Picard, V., Schweighoffer, F. and Der, C. J. (2008). Characterization of EHT 1864, a novel small molecule inhibitor of Rac family small GTPases. *Methods Enzymol.* **439**, 111-129.

Phng, L.-K., Gebala, V., Bentley, K., Philippides, A., Wacker, A., Mathivet, T., Sauteur, L., Stanchi, F., Belting, H.-G., Affolter, M. et al. (2015). Formin-mediated actin polymerization at endothelial junctions is required for vessel lumen formation and stabilization. *Dev. Cell* **32**, 123-132.

Price, L. S., Langeslag, M., ten Klooster, J. P., Hordijk, P. L., Jalink, K. and Collard, J. G. (2003). Calcium signaling regulates translocation and activation of Rac. *J. Biol. Chem.* **278**, 39413-39421.

Rossman, K. L., Der, C. J. and Sondek, J. (2005). GEF means go: turning on RHO GTPases with guanine nucleotide-exchange factors. *Nat. Rev. Mol. Cell Biol.* **6**, 167-180.

Sauteur, L., Krudewig, A., Herwig, L., Ehrenfeuchter, N., Lenard, A., Affolter, M. and Belting, H.-G. (2014). Cdh5/VE-cadherin promotes endothelial cell interface elongation via cortical actin polymerization during angiogenic sprouting. *Cell Rep.* **9**, 504-513.

Schulte, D., Küppers, V., Dartsch, N., Broermann, A., Li, H., Zarbock, A., Kamenyeva, O., Kiefer, F., Khandoga, A., Massberg, S. et al. (2011). Stabilizing the VE-cadherin-catenin complex blocks leukocyte extravasation and vascular permeability. *EMBO J.* **30**, 4157-4170.

Spindler, V., Schlegel, N. and Waschke, J. (2010). Role of GTPases in control of microvascular permeability. *Cardiovasc. Res.* **87**, 243-253.

Timmerman, I., Hoogenboezem, M., Bennett, A. M., Geerts, D., Hordijk, P. L. and van Buul, J. D. (2012). The tyrosine phosphatase SHP2 regulates recovery of endothelial adherens junctions through control of beta-catenin phosphorylation. *Mol. Biol. Cell* **23**, 4212-4225.

van Buul, J. D., Anthony, E. C., Fernandez-Borja, M., Burridge, K. and Hordijk, P. L. (2005). Proline-rich tyrosine kinase 2 (Pyk2) mediates vascular endothelial-cadherin-based cell-cell adhesion by regulating beta-catenin tyrosine phosphorylation. *J. Biol. Chem.* **280**, 21129-21136.

van Buul, J. D., Allingham, M. J., Samson, T., Meller, J., Boulter, E., Garcia-Mata, R. and Burridge, K. (2007). RhoG regulates endothelial apical cup assembly downstream from ICAM1 engagement and is involved in leukocyte trans-endothelial migration. *J. Cell Biol.* **178**, 1279-1293.

van Hinsbergh, V. W. M. and van Nieuw Amerongen, G. P. (2002). Intracellular signalling involved in modulating human endothelial barrier function. *J. Anat.* **200**, 549-560.

van Rijssel, J., Hoogenboezem, M., Wester, L., Hordijk, P. L. and van Buul, J. D. (2012a). The N-terminal DH-PH domain of Trio induces cell spreading and migration by regulating lamellipodia dynamics in a Rac1-dependent fashion. *PLoS ONE* **7**, e29912.

van Rijssel, J., Kroon, J., Hoogenboezem, M., van Alphen, F. P., de Jong, R. J., Kostadinova, E., Geerts, D., Hordijk, P. L. and van Buul, J. D. (2012b). The Rho-guanine nucleotide exchange factor Trio controls leukocyte transendothelial migration by promoting docking structure formation. *Mol. Biol. Cell.* **23**, 2831-2844.

Van Rijssel, J., Timmerman, I., Van Alphen, F. P. J., Hoogenboezem, M., Korchynskyi, O., Geerts, D., Geissler, J., Reedquist, K. A., Niessen, H. W. M. and Van Buul, J. D. (2013). The Rho-GEF Trio regulates a novel pro-inflammatory pathway through the transcription factor Ets2. *Biol. Open* **2**, 569-579.

van Wetering, S., van Buul, J. D., Quik, S., Mul, F. P., Anthony, E. C., ten Klooster, J. P., Collard, J. G. and Hordijk, P. L. (2002). Reactive oxygen species mediate Rac-induced loss of cell-cell adhesion in primary human endothelial cells. *J. Cell Sci.* **115**, 1837-1846.

Verma, S., Shewan, A. M., Scott, J. A., Helwani, F. M., den Elzen, N. R., Miki, H., Takenawa, T. and Yap, A. S. (2004). Arp2/3 activity is necessary for efficient formation of E-cadherin adhesive contacts. *J. Biol. Chem.* **279**, 34062-34070.

Vestweber, D., Winderlich, M., Cagna, G. and Nottebaum, A. F. (2009). Cell adhesion dynamics at endothelial junctions: VE-cadherin as a major player. *Trends Cell Biol.* **19**, 8-15.

Wilson, C. W., Parker, L. H., Hall, C. J., Smyczek, T., Mak, J., Crow, A., Posthuma, G., De Mazière, A., Sagolla, M., Chalouni, C. et al. (2013). Rasip1 regulates vertebrate vascular endothelial junction stability through Epac1-Rap1 signaling. *Blood* **122**, 3678-3690.

Wittchen, E. S. and Burridge, K. (2008). Analysis of low molecular weight GTPase activity in endothelial cell cultures. *Methods Enzymol.* **443**, 285-298.

Yamada, S. and Nelson, W. J. (2007). Localized zones of Rho and Rac activities drive initiation and expansion of epithelial cell-cell adhesion. *J. Cell Biol.* **178**, 517-527.

Yamazaki, D., Oikawa, T. and Takenawa, T. (2007). Rac-WAVE-mediated actin reorganization is required for organization and maintenance of cell-cell adhesion. *J. Cell Sci.* **120**, 86-100.

Yano, T., Yamazaki, Y., Adachi, M., Okawa, K., Fort, P., Uji, M., Tsukita, S. and Tsukita, S. (2011). Tara up-regulates E-cadherin transcription by binding to the Trio RhoGEF and inhibiting Rac signaling. *J. Cell Biol.* **193**, 319-332.

Yap, A. S. and Kovacs, E. M. (2003). Direct cadherin-activated cell signaling: a view from the plasma membrane. *J. Cell Biol.* **160**, 11-16.

Zhang, J., Betson, M., Erasmus, J., Zeikos, K., Bailly, M., Cramer, L. P. and Braga, V. M. M. (2005). Actin at cell-cell junctions is composed of two dynamic and functional populations. *J. Cell Sci.* **118**, 5549-5562.

Supplemental Figures

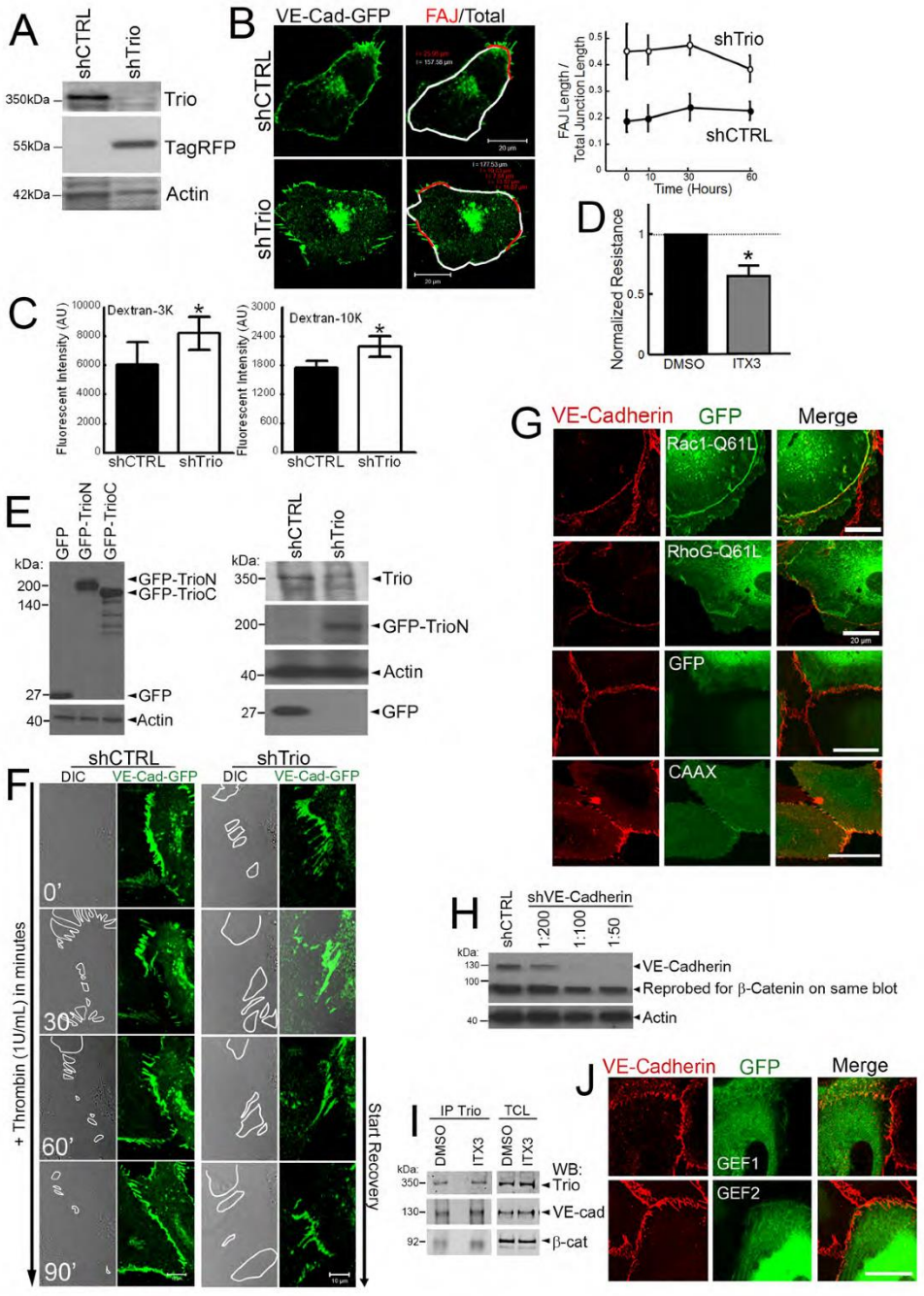

Figure S1. *Trio controls endothelial barrier function.* **(A)** TagRFP-shTrio constructs were expressed in ECs. Western blot shows efficient Trio knockdown in TagRFP-expressing ECs. **(B)** ECs, transiently transfected with VE-cadherin-GFP and treated with shCTRL or shTrio, are analyzed for FAJ length. Red line represents FAJ length and white line represents linear junction. When VE-cadherin staining showed zigzag pattern, it was quantified as FAJ. Graph on the right shows quantification of ratio between FAJ length and total junction length. Experiment is carried out three times independently from each other and 25 cells per experiment are analyzed. Data are mean±SEM. **(C)** Permeability was measured by culturing HUVECs on FN-coated Transwell filters and fluorescently-labeled Dextran was allowed to diffuse through the monolayer for four hours. Both dextran 3K and 10K showed increased permeability across Trio-deficient ECs. This experiment is carried out three times in duplicate. Data are mean±SD. *$p<0.05$. **(D)** ECs were cultured on FN-coated ECIS arrays and treated with ITX3 (100µM) or DMSO. Resistance was determined after 10h treatment and showed decreased resistance. Experiment is carried out three times independently from each other. Data are mean±SEM. *$p<0.01$. **(E)** Western blot analysis on the left shows efficient overexpression of GFP, GFP-TrioN and GFP-TrioC in endothelial cells. Blots on the right show expression of GFP-TrioN or GFP only in Trio-deficient endothelial cells. Actin is shown as loading control. **(F)** Intercellular gaps are quantified based on DIC images. shCTRL or shTrio-HUVECs were transfected with VE-Cadherin-GFP and 1U/mL Thrombin was administered for time periods (minutes) indicated in left lower corner. Stills show the gap size, illustrated with the white line. Bar: 10 µm. **(G)** ECs were cultured on FN-coated glass covers, transfected as indicated, stained. The constitutively active mutant of RhoG (Q61L), GFP-CAAX or GFP do not co-localize with VE-cadherin (red), whereas constitutively active Rac1 (Q61L) does co-localize with VE-cadherin. Bar: 20 µm. **(H)** Western blot confirms efficient VE-cadherin knock down. For the experiment, 1:50 dilution was used. The same blot was re-probed for β-catenin . Actin is used as loading control. **(I)** Trio-GEF1 activity is not required for its interaction with the VE-cadherin complex. DMSO- or ITX3-treated HUVECs were lysed and subjected to an IP for Trio. **(J)** ECs were cultured on FN-coated glass covers, transfected as indicated, stained. The N-terminal GEF1 domain of Trio (GEF1) as well as the C-terminal GEF domain of Trio (GEF2) do not show clear co-localization with VE-cadherin (red). Bar: 20 µm.

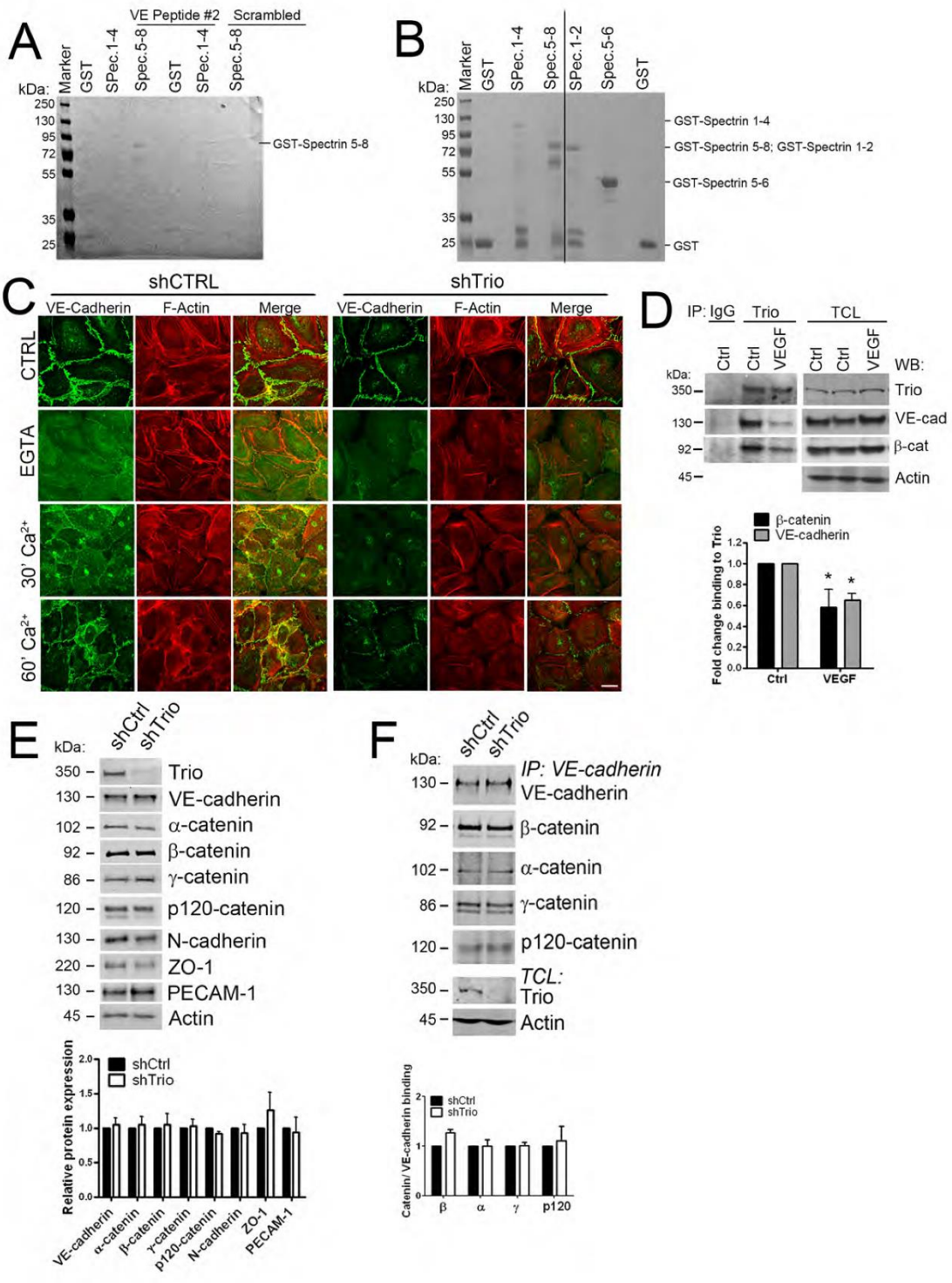
A
VE Peptide #2
Scrambled
Marker
GST
SPec.1-4
Spec.5-8
GST
SPec.1-4
Spec.5-8
kDa:
250
130
95
72
55
35
25
GST-Spectrin 5-8
B
Marker
GST
SPec.1-4
Spec.5-8
SPec.1-2
Spec.5-6
GST
GST-Spectrin 1-4
GST-Spectrin 5-8; GST-Spectrin 1-2
GST-Spectrin 5-6
GST
C
shCTRL
shTrio
VE-Cadherin
F-Actin
Merge
CTRL
EGTA
30' Ca2+
60' Ca2+
D
IP: IgG
Trio
TCL
Ctrl
Ctrl
VEGF
WB:
Trio
VE-cad
β-cat
Actin
β-catenin
VE-cadherin
Fold change binding to Trio
Ctrl
VEGF
E
shCtrl
shTrio
Trio
VE-cadherin
α-catenin
β-catenin
γ-catenin
p120-catenin
N-cadherin
ZO-1
PECAM-1
Actin
Relative protein expression
F
IP: VE-cadherin
TCL:
Catenin/ VE-cadherin binding
β
α
γ
p120

Figure S2. *Trio interacts with VE-cadherin.* **(A)** GST-spectrin-repeats 1-4 and 5-8 and GST alone were incubated with VE #2 or scrambled peptide as indicated. Western blot analysis shows that spectrin-repeats 5-8 bound to the VE and not to the scrambled peptide. **(B)** Western blot shows the input of the GST proteins as indicated for pull down experiments in Figure 4G and S2A. **(C)** Trio-deficient (shTrio) or control (shCTRL) ECs were treated with 4mM EGTA as indicated to chelate calcium and calcium (1mM $CaCl_2$) was added back for 30-60 min. Cells were stained as indicated. Bar: 20 μm. **(D)** ECs were grown to confluence and stimulated with 50ng/mL VEGF for 30 min. Cells were lysed and subjected to Trio IP. Association of VE-cadherin and β-catenin to Trio was determined by Western blotting. Quantification of three independent experiments is shown in lower panel. Data are mean±SEM. *$p<0.05$. **(E)** ECs were transduced with control or Trio shRNA, grown to confluency and lysed. Expression levels of several junction markers were determined by Western Blotting. Quantification of three independent experiments is shown in lower panel. **(F)** ECs were transduced with control or Trio shRNA, grown to confluency, lysed and an immunoprecipitation (IP) for VE-cadherin was performed. Blot shows that binding of catenins to VE-cadherin is not altered in Trio-depleted cells. Quantification of three independent experiments is shown in lower panel.

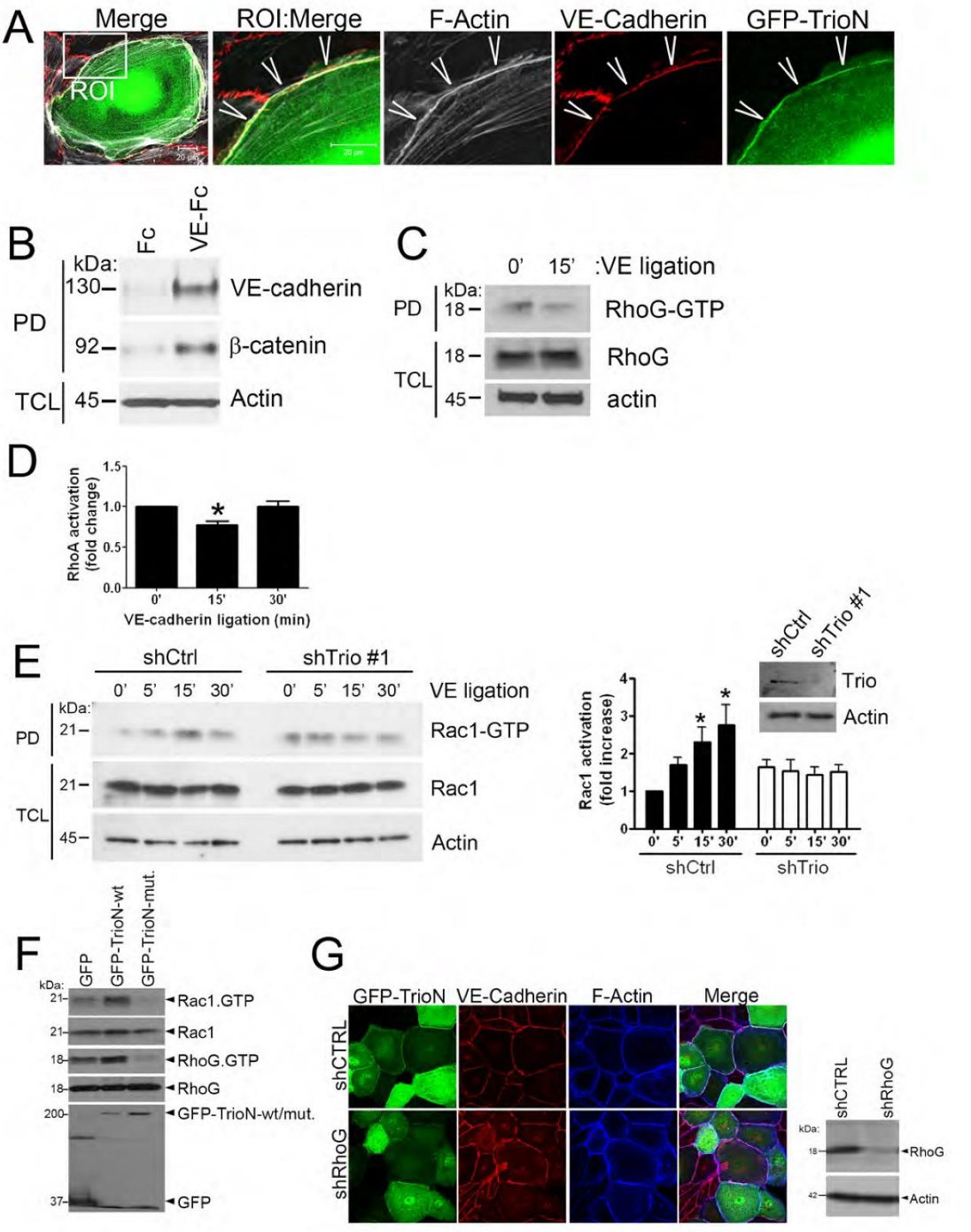
A
Merge
ROI:Merge
F-Actin
VE-Cadherin
GFP-TrioN
ROI
B
Fc
VE-Fc
kDa:
130
92
45
PD
TCL
VE-cadherin
β-catenin
Actin
C
0'
15'
:VE ligation
kDa:
18
18
45
PD
TCL
RhoG-GTP
RhoG
actin
D
RhoA activation (fold change)
1.5
1.0
0.5
0.0
0'
15'
30'
VE-cadherin ligation (min)
E
shCtrl
shTrio #1
0' 5' 15' 30'
0' 5' 15' 30'
VE ligation
kDa:
21
21
45
PD
TCL
Rac1-GTP
Rac1
Actin
shCtrl
shTrio #1
Trio
Actin
Rac1 activation (fold increase)
4
3
2
1
0
0' 5' 15' 30'
0' 5' 15' 30'
shCtrl
shTrio
F
GFP
GFP-TrioN-wt
GFP-TrioN-mut.
kDa:
21
21
18
18
200
37
Rac1.GTP
Rac1
RhoG.GTP
RhoG
GFP-TrioN-wt/mut.
GFP
G
GFP-TrioN
VE-Cadherin
F-Actin
Merge
shCTRL
shRhoG
shCTRL
shRhoG
kDa:
18
42
RhoG
Actin

Figure S3. *Trio promotes linear F-actin-rich cell-cell junctions and Rac1 activation.* **(A)** ECs were cultured on FN-coated glass covers, transfected with GFP-TrioN and stained as indicated. Region of interest (ROI) shows increase in F-actin at cell-cell junctions. Bar: 20 μm. **(B)** VE-cadherin-ectodomain-Fc- or Fc-coated magnetic dyna-beads were added to an EC monolayer to induce VE-cadherin ligation. ECs were lysed and adhered beads were isolated using a magnetic holder. Binding of endogenous VE-cadherin and β-catenin to the beads was determined by Western blotting. **(C)** VE-cadherin ligation does not increase RhoG activation, as analyzed using a GST-ELMO pull-down assay. **(D)** RhoA activation was analyzed using a G-LISA kit and showed a significant decrease in RhoA activation upon VE-cadherin ligation. Experiment is carried out three times. Data are mean±SEM. *$p<0.05$. **(E)** HUVECs were transduced with control or Trio shRNA #1 and incubated with VE-cadherin-ectodomain-Fc-coated magnetic beads to induce VE-cadherin ligation. Right panels show quantification, including Western blot control for Trio knockdown. Data are mean±SEM. *$p<0.05$. **(F)** HEK293 cells were transfected with GFP, GFP-TrioN-wt or GFP-TrioN-1406A/D1407A and Rac1 and RhoG activity was measured as described in the Method section. The catalytic-dead mutant N1406A/D1407A of TrioN showed no increase in Rac1 activation. Upper panel shows GTPase activity after pull down and panels below show total cell lysates and protein loading. Experiment is carried out three times independently from each other. (G) HUVECs were cultured to confluency and RhoG was silenced using shRNA as indicated. GFP-TrioN was overexpressed and localized to cell-cell junctions. Cells were fixed, permeabilized and stained for VE-cadherin in red, F-actin in blue. Merge shows co-localization between GFP-Trio, VE-cadherin and F-actin. RhoG depletion did not affect TrioN-induced linearization of cell-cell junctions. Western blot analysis showed efficient RhoG knock down (shRhoG) in HUVECs. Actin is shown as loading control. Previous work from our group showed that this shRNA did not affect Rac1 levels (Van Rijssel et al., MBoC 2012).

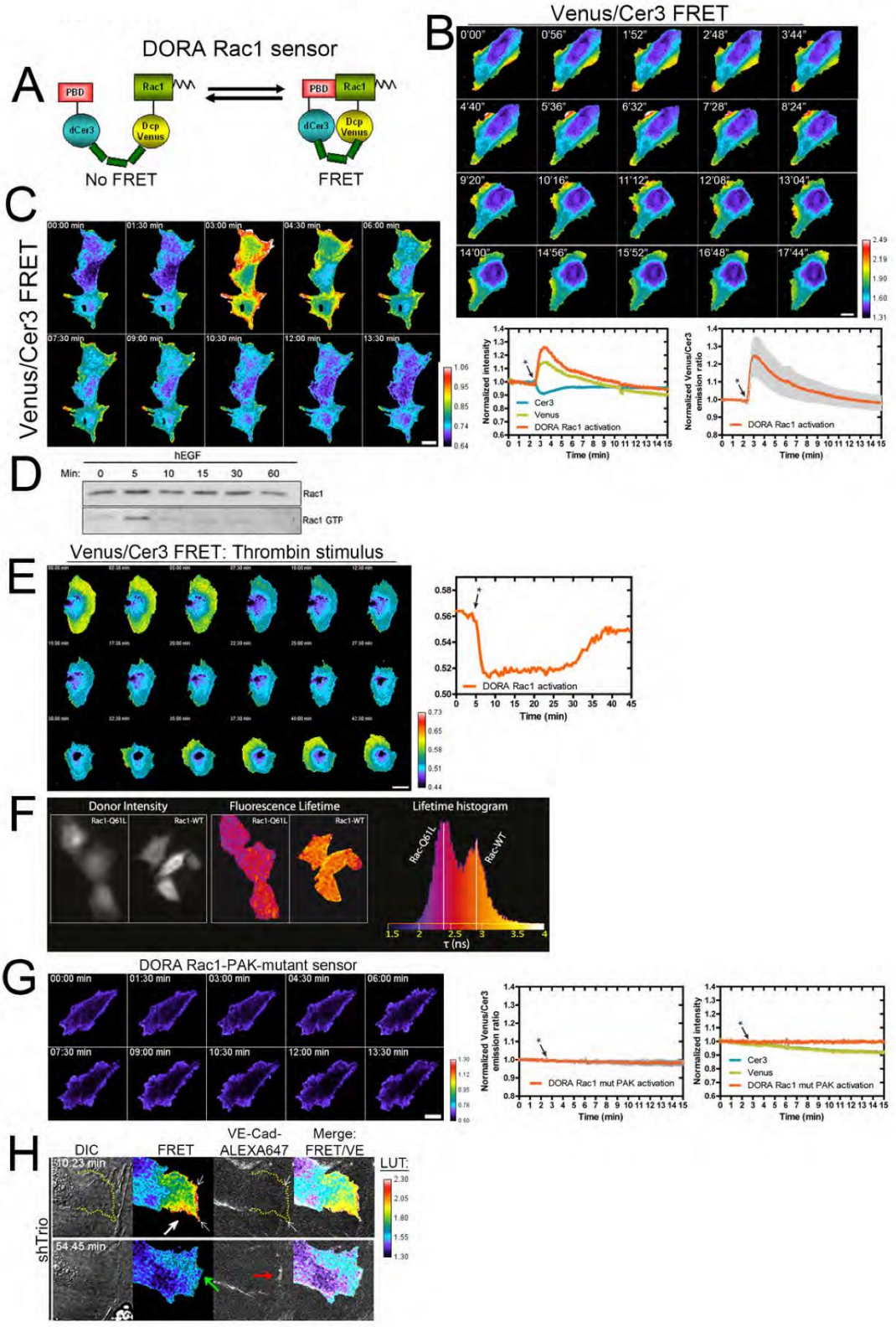
A
DORA Rac1 sensor
PBD
Rac1
dCer3
Dcp Venus
No FRET
FRET
B
Venus/Cer3 FRET
0'00"
0'56"
1'52"
2'48"
3'44"
4'40"
5'36"
6'32"
7'28"
8'24"
9'20"
10'16"
11'12"
12'08"
13'04"
14'00"
14'56"
15'52"
16'48"
17'44"
Normalized intensity
Cer3
Venus
DORA Rac1 activation
Time (min)
Normalized Venus/Cer3 emission ratio
C
Venus/Cer3 FRET
00:00 min
01:30 min
03:00 min
04:30 min
06:00 min
07:30 min
09:00 min
10:30 min
12:00 min
13:30 min
D
hEGF
Min: 0 5 10 15 30 60
Rac1
Rac1 GTP
E
Venus/Cer3 FRET: Thrombin stimulus
DORA Rac1 activation
Time (min)
F
Donor Intensity
Fluorescence Lifetime
Lifetime histogram
Rac1-Q61L
Rac1-WT
τ (ns)
G
DORA Rac1-PAK-mutant sensor
DORA Rac1 mut PAK activation
H
DIC
FRET
VE-Cad-ALEXA647
Merge: FRET/VE
LUT:
shTrio
10.23 min
54.45 min

Figure S4. *Quantification of DORA Rac1 sensor*. **(A)** Schematic drawing of the Rac1 single-chain DORA sensor. Rac1-wt and the Pak-binding domain (PBD) are both located at the outside of the sensor. Cerulean3 and Venus are used to generate FRET when Rac1 and PBD are in close proximity. Both parts are linked through the ribosome linker protein L9, ensuring low off-rate FRET. **(B)** Stills from Movie 5 (left) showing spontaneous protrusions of Rac1 DORA sensor transfected ECs with spatial and temporal Rac1 activation at protrusions. Heat map (LUT) on the right shows FRET ratio. Warm colors indicate FRET. **(C)** HeLa cells were transfected with the Rac1 sensor and stimulated with EGF (concentration; arrow/asterisk) for indicated time points. Rac1 activity, as result of FRET, was shown in warm colors according to the heat map and showed transient activation upon EGF treatment. Right graph shows normalized intensity of Cerulean (blue) and Venus (yellow) and red line indicates transient increased FRET (YFP/CFP) ratio upon EGF (asterisk). Second most right graph shows average of three independent experiments of FRET ratio upon EGF treatment. **(D)** Western blot analysis of Rac1 activity upon EGF reflects FRET data presented under C. **(E)** ECs transfected with DORA Rac1 sensor were stimulated with thrombin (1U/mL; arrow/asterisk). Rapid decrease in FRET signals was detected, followed by a local increase in FRET signal during the recovery phase. Warm colors indicate increased FRET. Graph on the right shows FRET ratio. **(F)** Quantitative imaging of active and wt Rac1 biosensor by fluorescence lifetime imaging (FLIM). Reduced FLIM of the constitutively active Rac1 (Q61L) sensor mutant compared to the Rac1-wt sensor was measured, indicating efficient FRET. **(G)** Dominant negative DORA Rac1-PAK-mutant sensor shows no increase in FRET, indicating low background sensor signals. Also the graphs on the right show no change in fluorescent intensity for Cerulean, Venus or FRET ratio. **(H)** Trio-deficient ECs (marked by TagRFP-shTrio) show high FRET signals, reflecting Rac1 activity at the front of a protrusion (white arrow). However, upon initial cell-cell contact, marked by VE-cad-647 (red arrow), no increase in FRET is measured (green arrow). LUT: heat map on right shows warm colors as high FRET.

Movies

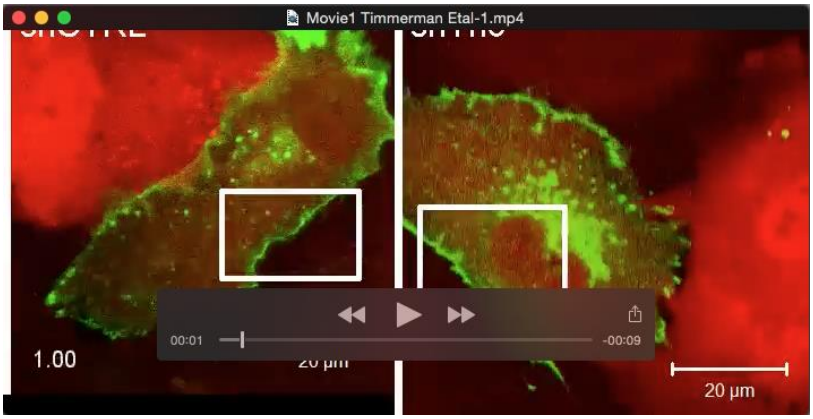

Movie 1. Related to figure 1. Time-lapse recording of HUVECs expressing VE-cadherin-GFP and Tag-RFP-shCTRL (left) or Tag-RFP-shTrio (right). Movie shows EC monolayer dynamics for 30 minutes. Images were taken every 30 seconds. Box represents ROI shown in Figure 1A.

Movie 2. Related to figure 2. Time-lapse recording of thrombin-stimulated HUVECs expressing VE-cadherin-GFP and RFP-Lifeact. Movie shows retracting endothelial cells upon thrombin (1U/mL) stimulation, followed by recovery phase and re-assembly of cell-cell junctions. Timeframe of the movie is 1.5 hours and images were taken every 16 seconds.

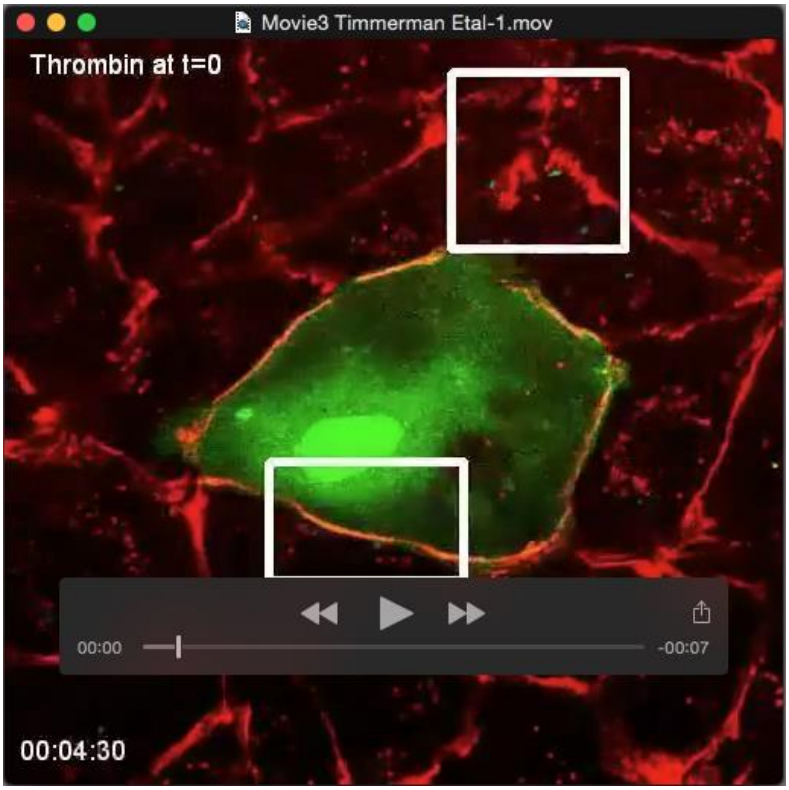

Movie 3. Related to figure 2. Time-lapse recordings showing linear stable cell-cell junctions in GFP-Trio-N (N-terminus) expressing cells after thrombin stimulation (arrowheads), whereas a major part of cell-cell junctions of non-transfected cells are disrupted (arrows). VE-cadherin is visualized using an Alexa-647-conjugated VE-cadherin antibody. Timeframe of the movie is 75 minutes and images were taken every 45 seconds.

Movie 4. Related to figure 2. Time-lapse recording of thrombin-stimulated shCTRL- (left) or shTrio- (right) treated HUVECs expressing VE-cadherin-GFP. Movie shows disruption of VE-cadherin-based cell-cell junctions (white and red arrows), followed by junction recovery. In control conditions, recovery results in linear junction morphology (yellow arrows). In shTrio ECs, junctions first recover (arrowheads) but disassemble rapidly after (red arrows). Timeframe of the movie is 150 minutes and images were taken every 30 seconds.

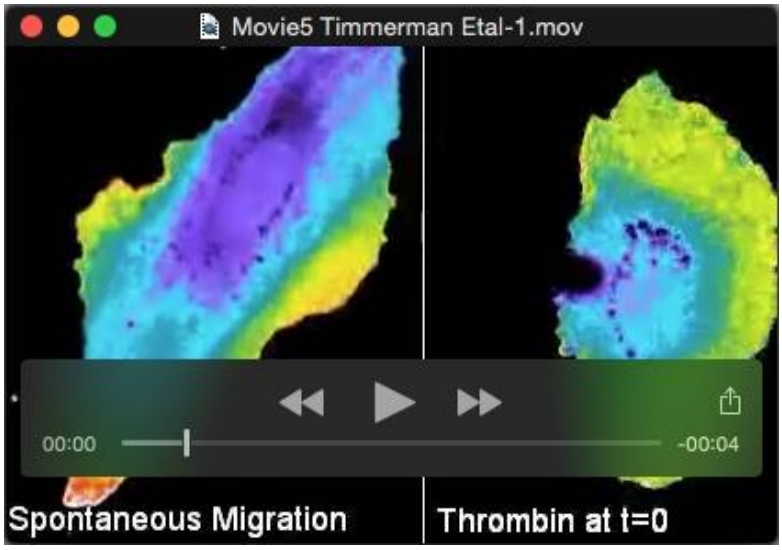

Movie 5. Related to figure 7. Time-lapse movie of a Rac1 DORA-biosensor-expressing endothelial cell making spontaneous membrane protrusions (left) or stimulated with thrombin (1U/mL) (right). Note the high FRET ratio and the rapid on and off state of the sensor, comparable with the formation and contraction of the membrane protrusions. See for LUT, figure S4B,E. Timeframe of the left movie is 20 minutes and images were taken every 5 seconds. Timeframe of the right movie is 45 minutes and images were taken every 30 seconds.

Movie 6. Related to figure 7. Time-lapse movie of a Rac1 DORA-biosensor-expressing endothelial cell making cell-cell contact with a non-expressing cell. Movie panel on the left shows DIC with time indication and white arrow shows initial cell-cell contact. FRET signal of Venus/Cerulean3 at cell-cell junction regions is indicated by arrowheads, α-catenin-mCherry (α-Cat) upon junction formation is shown by white arrows and the merge of Rac1 activity (FRET signal) with α-catenin-mCherry is depicted in the right frame. At the right, the color bar represents FRET ratio with warm colors as the highest signal. Arrowheads indicate local FRET signals upon the formation of cell-cell contact. Timeframe of the movie is 44 minutes and images were taken every 8 seconds.

Movie 7. Related to figure 7. Time-lapse movie of Trio-deficient endothelial cells expressing the Rac1-biosensor and VE-cadherin-ALEXA-647 in an attempt to re-assemble cell-cell contact. Movie panel on the left shows DIC with time indication, and white arrows indicating dis- and re-assembly of cell-cell junctions; second panel shows FRET signal of Venus/Cerulean3, and arrowheads show FRET for cell-cell junction selected region; third panel shows VE-cadherin-ALEXA-647 as cell-cell junction marker in white and fourth panel shows the merge of Rac1 activity (FRET signal) in red with VE-cadherin in green. At the right, the color bar represents FRET ratio with warm colors as the highest signal. Timeframe of the movie is 60 minutes and images were taken every 16 seconds.

Movie 8. Related to figure 7. Time-lapse movie of Trio-deficient endothelial cells expressing the Rac1-biosensor and VE-cadherin-ALEXA-647. Movie panel on the left shows DIC with time indication; second panel shows FRET signal of Venus/Cerulean3, third panel shows VE-cadherin-ALEXA-647 as cell-cell junction marker in white and fourth panel shows the merge of Rac1 activity (FRET signal) with VE-cadherin. At the right, the color bar represents FRET ratio with warm colors as the highest signal. White arrows show local Rac1 activity upon the induction of spontaneous protrusions in the absence of VE-cadherin. Green and red arrow show the formation of cell-cell contact, marked with VE-cadherin, and an absence of FRET signal. Timeframe of the movie is 90 minutes and images were taken every 20 seconds.